Reviewer 1

General comments

This paper compares SP-AMS and AMS data at an urban location in the US to infer details concerning the behaviour of black carbon aerosols and SOA formation in this environment. This is partly facilitated by the dataset exhibiting a strong diurnal profile, meaning that traits can be reported with decent statistical power, in spite of the sampling period being relatively short. While the quantitative accuracy of the SP-AMS may be questionable (many of the RIEs and CEs are simply assumed rather than calibrated here), this does not form the major part of the science. This paper is well written and has the potential to provide some useful insight relevant to ACP, however I feel that the discussion side of the paper needs more work. Specifically, the authors appear to be making two unsafe assumptions often inappropriately made when analysing data of this nature; firstly, they seem to be assuming that the patterns are governed by sources and in situ processes (neglecting advection), akin to a box model and second, they seem to be treating the PMF factors as discrete chemical entities. While I'm sure the authors are aware of the issues here, this is not currently reflected in the text and a few conclusions are made that I would regard as unsafe. I recommend that this be published subject to major corrections.

Response: We thank for the reviewer's comments. We agree with the reviewer that the original version did not clearly reflect the potential impacts of advection on our diurnal observations. Furthermore, as the reviewer suggested in the specific comments, OOA factors identified by PMF analysis are combined in the revised version in order to provide more objective interpretation and comparison between the two AMS measurements. The manuscript has been revised accordingly throughout the discussion as highlighted in the specific comments below.

Specific comments

There an issue that I can see regarding the conclusions of the comparison of organic factors from the two AMSs in that the authors appear to be treating the PMF-derived SOA factors as discrete chemical types. While this could hypothetically be the case, it is far more likely that when applying the simple PMF data model to a chemically complex system such as this, the two SOA factors for each instrument represent the mathematical endpoints of a distribution of data, within the non-negativity constraint imposed. This being the case, a direct comparison of the two instruments' factors may be problematic; given that it is known their mass spectral responses to different organic materials are fundamentally different, their respective factorisations could end up being very different in character for the same aerosol simply through virtue of how the spectra are distributed in multivariate space and what endpoints are converged on by the solver. As a suggestion, a more objective comparison of the two datasets might be achieved if the primary factors (determined using PMF) are subtracted from the data matrices then metrics such as elemental ratios derived from what is left (assuming it is all secondary), e.g. as new points on figure 7. See https://www.atmos-chem-phys.net/15/6351/2015/.

Response:

We agree with the reviewer that comparison of total OOA measured by the two instruments may be more objective. Similar to Figure 6 in the original version, we have included the comparison of total OOA measured by both AMS instruments (i.e. $SOA_{NR\text{-}PM}$ = NOOA + VOOA for HR-ToF-

AMS and SOA_{rBC} = OOA-1 and OOA-2 for SP-AMS) in Figure 7 as suggested by the reviewer. Note that signals of organic fragments at m/z 30 and 46 were removed from the updated PMF input due to the significant interferences of nitrate fragments to these organic fragments (Chen et al., submitted). With the updated results of PMF analysis (see Figure S6 in SI), Figures 6 and 7 have been modified accordingly in the revised manuscript. The results presented in Figure 6 are similar to those reported in the original version. Discussion for Figure 7 has been modified as shown below:

Page 9: “The elemental ratios (O/C and H/C) extracted from the SP-AMS and HR-ToF-AMS mass spectra of oxidized organic species have been shown to be different. Canagaratna et al. (2015b) reported that the SP-AMS O/C and H/C values differ from their corresponding HR-ToF-AMS values by factors of 0.83 and 1.16, respectively, based on the laboratory analysis of chemical standards, including dicarboxylic acids, multifunctional acids and alcohols. These conversion factors are applied to the O/C and H/C ratios of NOOA, VOOA and SOA_{NR-PM} (i.e., mass-weighted values of NOOA and VOOA) (Chen et al., 2017) in order to perform a more meaningful comparison to our SP-AMS measurements in the Van Krevelen diagram (Figure 7). The elemental ratios of SOA_{rBC} and SOA_{NR-PM} are comparable to each other, well within the measurement uncertainties. Similar observations are obtained between OOA-2 and VOOA. In contrast, the O/C and H/C ratios of OOA-1 are rather different to the adjusted values of NOOA, VOOA and SOA_{NR-PM}, suggesting some chemical difference between OOA-1 and those SOA materials. This is also consistent with the fact that OOA-1 mass concentrations increased faster than other OOA materials in the morning. More field and laboratory data are required to validate and improve the empirical relationships proposed by Canagaratna et al., (2015b) and to understand the extent to which the observed differences are a result of true chemical differences versus explainable by differences in molecular fragmentation due to the different vaporization schemes used in the instruments.”

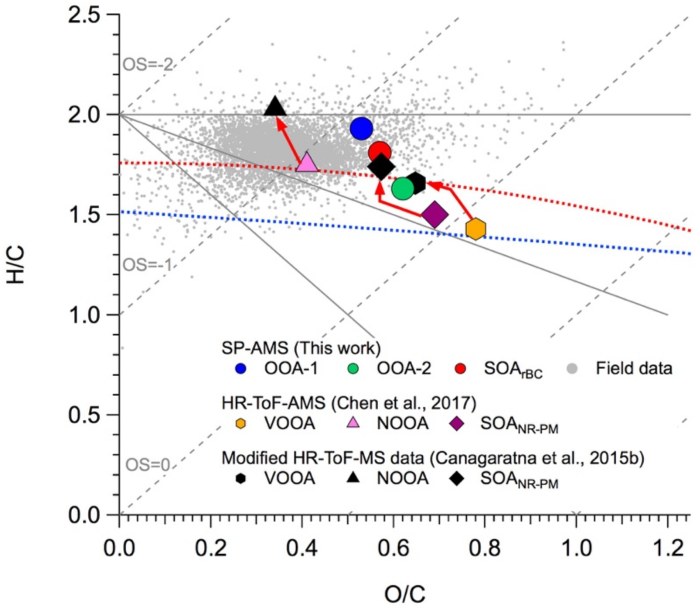

Figure 7: Van Krevelen diagram: Red arrows indicate the changes in the elemental ratios of VOOA, NOOA factors and SOA_{NR-PM} measured by the HR-ToF-AMS after applying the correction factors for more oxygenated organic species proposed by Canagaratna et al. (2015b).

In addition, we have combined the diurnal variations of OOA factors as shown in the revised Figure 5g (i.e., SOA_{rBC} vs. $SOA_{NR\text{-}PM}$). Discussions for Figure 5g has been modified as shown below:

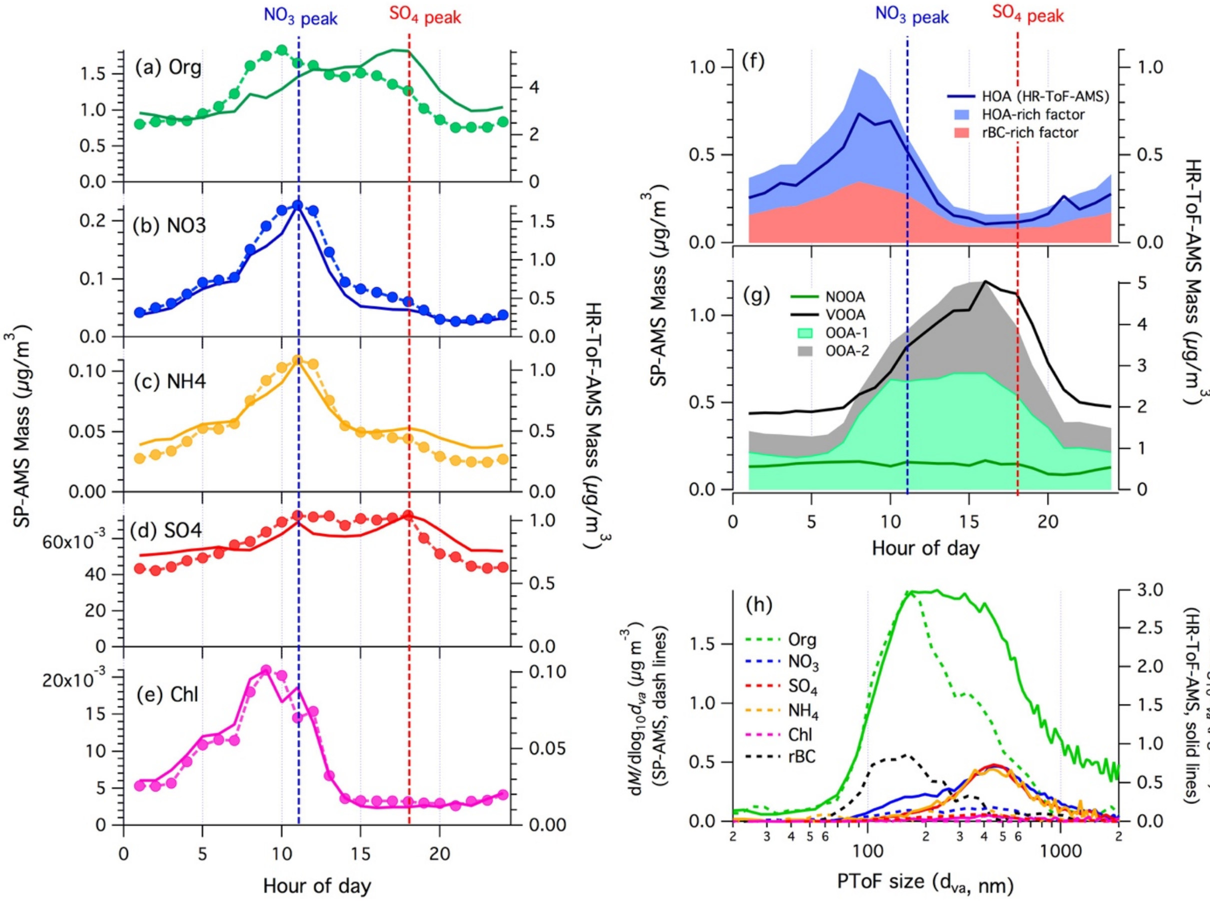

Figure 5: (a-e) Diurnal cycles of NR-PM and $NR\text{-}PM_{rBC}$ measured by HR-ToF-AMS (solid lines) and SP-AMS (dashed lines with circles), respectively. (f-g) Diurnal cycles of PMF factors from HR-ToF-AMS (solid lines) and SP-AMS (filled areas, organics components only for PMF factors) data. (h) PToF size distribution of rBC, NR-PM (dashed lines) and $NR\text{-}PM_{rBC}$ (solid lines).

Page 8: "SOA was the most abundant OA component. VOOA and NOOA accounted for 60 and 17 wt% of total OA in NR-PM, respectively. Diurnal variations of NOOA were minimal, whereas VOOA mass concentrations increased continuously from ~8:00 and peaked at ~18:00 (Figures 5g and S6). Although PMF analysis identified two SOA factors for both AMS measurements, the total SOA concentrations were calculated to provide overall comparisons of SOA mass loadings in NR-PM and $NR\text{-}PM_{rBC}$ regardless their sources. Specifically, $SOA_{NR\text{-}PM}$ = NOOA + VOOA for HR-ToF-AMS and SOA_{rBC} = OOA-1 and OOA-2 for SP-AMS. The average $SOA_{rBC}/SOA_{NR\text{-}PM}$ is equal to 0.2, indicating that approximately 20 wt% of OOA components were internally mixed with rBC on average during the hot period (Figure 6). It is worth noting that SOA_{rBC} increased at a faster rate in the morning compared to $SOA_{NR\text{-}PM}$, suggesting that SOA_{rBC} and $SOA_{NR\text{-}PM}$ could be produced or transported from different sources, at least to some extent. Furthermore, $SOA_{NR\text{-}}$

$_{PM}$ mass concentrations started dropping substantially at ~18:00-19:00, which was about 1-2 hours delay compared to SOA$_{rBC}$ (Figure 5g). This observable delay corresponded to the time of increasing sulfate levels in NR-PM, implying potential sources and formation pathways of VOOA (i.e., the major component of SOA$_{NR-PM}$ within that period) that might be related to the regional transport of aged particles. This possible explanation is consistent with the observation that VOOA represented more oxidized OOA materials (i.e. more aged) and that the strongest average wind speed was observed at around 18:00-19:00 (Figure 2c). Single particle measurements using the light scattering module of the HR-ToF-AMS also suggests internal mixing of sulfate and highly oxidized OOA materials in NR-PM (Chen et al., 2017). Nevertheless, VOOA could also be produced through local photochemistry as 1) it was unlikely that all the locally formed SOA materials were condensed on rBC particles exclusively during the day and 2) the HR-ToF-AMS should be able to detect OOA-1 and OOA-2 materials as well. The relative contributions of local photochemistry and regional transport to the observed VOOA mass could not be separated by the PMF analysis possibly due to the chemical similarity of those SOA materials."

An entire line of discussion – comparing the behaviour of organics to sulphate – I consider to be deeply flawed in the way it has been approached here. Outside of aqueous-phase processing (which is almost certainly not happening here, given the low humidities), the formation lifetime of sulphate from the gas phase oxidation of sulphur dioxide tends to occur on the timescale of weeks (far beyond the timescale where NOy/NOx is a useful indicator of photochemistry), which means that a diurnal pattern observed here is extremely unlikely to be a manifestation of the chemistry. I would consider it far more likely that the relatively modest pattern that does exist (noting that the vertical axes in figure 5d are not scaled from zero) is caused by the transport of regional pollution or marine air into the area during the day and concentrations decreasing at night through dry deposition in the nocturnal inversion layer, consistent with the wind speeds. It may also be that an analogous process, driven by dynamical rather than chemical processes, may be occurring for the highly oxidised SOA.

Response:

The sentence has been revised as shown below to address the possibility of regional transport of sulfate during the day.

Page 6: "Sulfate remained in low concentrations with relatively modest pattern (see also Figure 5d) potentially caused by the transport of regional pollution into the area during the day."

Furthermore, the above information has been integrated to the discussion regarding the potential sources of VOOA (i.e. more oxidized OOA materials) as shown below:

Page 8: "SOA$_{NR-PM}$ mass concentrations started dropping substantially at ~18:00-19:00, which was about 1-2 hours delay compared to SOA$_{rBC}$ (Figure 5g). This observable delay corresponded to the time of increasing sulfate levels in NR-PM, implying potential sources and formation pathways of VOOA (i.e., the major component of SOA$_{NR-PM}$ within that period) that might be related to the regional transport of aged particles. This possible explanation is consistent with the observation that VOOA represented more oxidized OOA materials (i.e. more aged) and that the strongest average wind speed was observed at around 18:00-19:00 (Figure 2c). Single particle measurements using the light scattering module of the HR-ToF-AMS also suggests internal mixing of sulfate and highly oxidized OOA materials in NR-PM (Chen et al., 2017)."

The third paragraph on page 8 makes a lot of very speculative statements concerning mechanisms that I do not consider to be adequately supported by the evidence and in certain cases implicitly rely on assumptions I do not consider safe. Not least of which is the tendency, as described in the general comments, to implicitly treat the factors represent discrete chemical types. But beyond this, I find the following lines of discussion to be problematic:

1) By using sulphate as a point of comparison for OOA, there is an intrinsic assumption that the precursors have similar sources on a regional level. While this is often the case at many sites, there are locations around the world (e.g. London) that do not conform to this behaviour. More evidence should be presented here that this is the case before drawing inferences concerning the chemical behaviour of these.

Response:

In this study, the HR-ToF-AMS was equipped with the light scattering module (LS-AMS), and thus single particle data was available to investigate the aerosol mixing state (Chen et al., submitted). By performing cluster analysis on the single particle data, it can be found that a portion of more- oxidized SOA materials were internally mixed with sulfate-rich particles. This provides direct evidence that at least a portion of VOOA materials were associated with the regional transport of sulfate. The aspect of internal mixing between VOOA and sulfate is addressed in the revised paragraph in our earlier response.

2) OOA-1 is described as being bimodal, however to my eyes, the trace in figure 5g simply has one very broad mode in its diurnal profile. Regardless, I fail to see how this constitutes evidence that there are different mechanisms in play in the morning versus the afternoon, so additional evidence to support this must be presented. Also see the comment concerning the treatment of SOA factors as discrete.

Response:

The sentences regarding bimodal pattern of OOA-1 have been removed in the revised version. Instead, we focus on discussing the diurnal patterns of total OOA measured by the two AMS measurements (see the response for the first specific comments), and the following sentence has been added for general description of OOA-1 factor in Section 3.2.

Page 6: "OOA-1 represented less oxygenated SOA components (O/C = 0.53) with 13.4 wt% of rBC content, and its concentration started increasing in the morning coincident with nitrate and ammonium (i.e., peaks at ~10:00-11:00, Figure 2a and 3g) and sustained at relatively constant levels until ~15:00–16:00."

3) While a factor may correlate with nitrate, I consider it too much of a jump to assume that they are mechanistically related. I consider it more likely that they are formed over similar timescales and/or have similar thermodynamic properties.

Response:

After modifying the discussion in this paragraph, the related sentences have been removed in the revised version.

Figure 5g: What are the red dashed lines?

Response:

The red dashed lines have been removed in Figure 5 due to the modified discussion for comparing SP-AMS and HR-ToF-AMS measurements.

Page 10: I would propose a much simpler explanation for the trends in the more highly oxidised material. If this is being formed regionally on longer timescales (as with sulphate), then this would already exist within the accumulation mode (which does not necessarily have to contain black carbon) and simply be advected in during the day. The less oxidised SOA formed more locally on shorter timescales could preferentially condense onto the BC particles through simple virtue of these Aiken mode particles presenting a larger overall surface area to the condensing gases. While it is hypothetically possible that there may be a mechanistic preference for material to condense onto certain surfaces because of their chemical nature, this would be a contentious statement to make and I do not see the data here as supportive of this notion.

Response:

The conclusion has been modified based on the suggestion from the reviewer. Even though we cannot provide direct evidence of a mechanistic preference for material to condense onto certain surfaces, we have changed our tone in the revised version to highlight this possibility for future research.

Page 10: "One of the possibilities is that $\mathrm{SOA_{rBC}}$ formed more locally on shorter timescales (e.g., photo-oxidation of anthropogenic volatile organic compounds (VOCs) near traffic emissions) could preferentially condense onto rBC particles in Aiken mode that can provide a larger overall surface area to the condensing gases compared to other existing background particles. The more oxidized OOA materials formed regionally on longer timescales (e.g., a fraction of VOOA that were largely externally mixed with rBC) under conditions with relatively low concentrations of (or without) rBC particle could be advected to the sampling region during the day. Furthermore, atmospheric dilution of traffic emissions can modify the chemical compositions and concentrations of SOA precursors and seed particles so that the formation of secondary coatings on rBC might be less efficient and chemically different under diluted conditions (e.g., after boundary layer break up and mixing with air masses from residual layer). This may partially explain the formation of

VOOA in SOA_{NR-PM} through local photochemistry. There may also be a mechanistic preference for material to condense onto certain surfaces because of their chemical nature (e.g., hydrophobic coating (e.g. HOA and soot surface functionality) but future research efforts are required to explore this possibility further. ”

Technical corrections:

Page 3, line 15: Which 42i was fitted with the photolytic converter? I assume the NOx instrument, but this should be explicit

Response: Yes, the photolytic converter was used for NO_x measurement. The sentence has been revised as following.

Page 3: “The heated molybdenum converter in the 42i nitrogen oxide analyzer was replaced by an UV-LED photolytic NO_2 converter (Air Quality Design) for NO_x measurement.”

Page 5, line 5: If the particle beam was found to be wider than the laser beam, this means that some particles may undergo incomplete vaporisation at the edges of the laser, which would in turn bias the measurement towards the coatings rather than the cores (see http://cires.colorado.edu/jimenezgroup/UsrMtgs/UsersMtg16/JDASPAMSfocusing.pdf). This should be added as a caveat.

Response: We agree that such measurement uncertainty should be included in the experimental section. The following sentence has been added to the revised manuscript (Page 5, lines 14-20):

Page 5: “The applied CE may be therefore less relevant for the time with high ambient SOA loading (i.e., high $NR\text{-}PM_{rBC}$/rBC mass ratio, or R_{BC}), leading to over quantification of the SOA components in $NR\text{-}PM_{rBC}$ by at most 40% due to this uncertainty. Furthermore, a wider particle beam than the laser beam implies that some rBC-containing particles may undergo incomplete vaporization at the edges of the laser vaporizer, which would in turn bias the measurement towards the coatings rather than the rBC cores (see unpublished data from, http://cires.colorado.edu/jimenezgroup/UsrMtgs/UsersMtg16/JDASPAMSfocusing.pdf). Since the CE of 0.6 was primarily determined for rBC, this phenomenon may further increase the degree of over quantification of $NR\text{-}PM_{rBC}$. Overall, the values of $NR\text{-}PM_{rBC}$ reported in this work likely represent their upper limits.”

Reviewer 2

Lee et al. investigated the mixing state of BC and the chemical characteristics of its coatings near vehicle emissions. They found that substantial formation of SOA coatings on BC particles was due to photochemistry in the afternoon, whereas POA was strongly associated with BC from fresh vehicular emissions in the morning rush hours. The paper potentially has significant implications to the formation of SOA coatings on BC in many urban environments, so is well within the scope for ACP. The paper is very interesting although some clarifications regarding the data analysis are required. The paper can be recommended for publication after the following questions are addressed.

Response: We thank for the reviewer of the positive comments.

General comments:

In Line 8-11, Page 5, the authors mentioned that CE for rBC particles increased (or rBC particle beam width decreases) with coating thickness. Although the variation of CE will not impact calculations of RBC, it will certainly influence the calculation of NR-PMrBC/NR-PM, which refers to the proportion of internally mixed aerosols. The authors should evaluate the impact of variable CEs on the calculation of NR-PMrBC/NR-PM.

Response:

We agree with the reviewer that we need to provide some information on the measurement uncertainties of NR-PM$_{rBC}$ in this work. As described in the manuscript and the literature, there are three major uncertainties for NR-PM$_{rBC}$ quantification: 1) CE of rBC-containing particles due to incomplete overlapping of particle and laser beams (Willis et al., 2014, page 5 lines 14-17 in the revised version), 2) IE calibration approach for laser vaporization scheme used in SP-AMS (Lee et al., 2015, page 5, lines 3-5), and 3) partial vaporization of particles at the edge of laser vaporizer that bias the measurement towards the coating rather than the rBC cores (unpublished data, http://cires.colorado.edu/jimenezgroup/UsrMtgs/UsersMtg16/JDASPAMSfocusing.pdf).

With the current estimation of CE=0.6 for all rBC-containing particles (point 1), NR-PM$_{rBC}$ of aged particles (i.e., those with high R$_{BC}$) may be over quantified by at most 40% (Willis et al., 2014). Lee et al. (2015) has illustrated that applying the standard mass-based IE calibration approach (point 2) may lead to over quantification of NR-PM$_{rBC}$ (i.e. apparent increased sensitivity to NR-PM$_{rBC}$ vaporized in laser vaporizer) for different types of particles measured by a SP-AMS equipped with dual vaporizers, and such uncertainty is likely instrument and vaporizer configuration dependent. Lastly, partial vaporization at the edge of laser vaporizer (point 3) results in a higher CE for NR-PM$_{rBC}$ than the rBC cores, leading to further over quantification of NR-PM$_{rBC}$ when CE correction factor of 0.6 is applied for all aerosol components. However, quantification of the overall uncertainties due to these major factors is not straightforward, and their importance have been clearly highlighted in the 17th AMS users meeting in 2016 after this field study (see summary slides prepared by Tim Onash from http://cires1.colorado.edu/jimenez-group/UsrMtgs/UsersMtg17/2015%20SP-AMS%20upate%20presentation%20-%20Onasch.pdf).

Even though the uncertainty of NR-PM$_{rBC}$ measurement cannot be accurately quantified in this work, the three major uncertainties lead to over quantification of NR-PM$_{rBC}$ in general, especially for those particles with high R$_{BC}$ (i.e. aged particles dominated by secondary inorganic and organic components). That means the NR-PM$_{rBC}$/NR-PM ratios reported in this work likely represent the upper limit. Including this additional information in the revised manuscript would not affect one of our major conclusions that only a small fraction of secondary organic and inorganic species were estimated to be internally mixed with rBC on average, implying that rBC is unlikely the major condensation sinks of SOA in this study.

Based on the comments from both reviewers, the original argument has been modified in the revised manuscript as shown below:

Page 5: "The applied CE may be therefore less relevant for the time with high ambient SOA loading (i.e., high NR-PM$_{rBC}$/rBC mass ratio, or R$_{BC}$), leading to over quantification of the SOA components in NR-PM$_{rBC}$ by at most 40% due to this uncertainty. Furthermore, a wider particle beam than the laser beam implies that some rBC-containing particles may undergo incomplete vaporization at the edges of the laser vaporizer, which would in turn bias the measurement towards the coatings rather than the rBC cores (see unpublished data from, http://cires.colorado.edu/jimenezgroup/UsrMtgs/UsersMtg16/JDASPAMSfocusing.pdf). Since the CE of 0.6 was primarily determined for rBC, this phenomenon may further increase the degree of over quantification of NR-PM$_{rBC}$. Overall, the values of NR-PM$_{rBC}$ reported in this work likely represent their upper limits."

In addition, gas-phase CO2 will contribute to the CO2+ signal and thus influence the chemical composition of OA (Aiken et al., 2007; Aiken et al., 2008). Was the contribution of gas-phase CO2 to CO2+ signal corrected in this study? This information was missing in the manuscript.

Response:

The contribution of gas-phase CO_2 to organic fragment CO_2^+ was determined by measuring the gas-phase CO_2 to N_2 ratio of particle-free ambient air. Such information has been added to the revised manuscript as shown below:

Page 4: "In particular, the average contribution of gas-phase CO_2 to CO_2^+ organic fragment in particle phase was determined (i.e., CO_2-to-N_2 ratio) based on the measurements of particle-free ambient air (i.e., at least 10 min per day) throughout the sampling period."

Specific comments:

Line 19-20, page 5: The data for SP-AMS on July 21 are not available, please give some clarifications.

Response: There were a few SP-AMS technical issues to be fixed from around July 20 18:00 to July 21 12:00. The following sentence has been added to the revised manuscript.

Page 5: "The SP-AMS was under maintenance from 20 July 18:00 to 21 July 12:00."

Line 26, page 5: What are the uncertainties of these items in Figure 2?

Response:

The major purpose of Figure 2 is to illustrate the diurnal trend of each species during the hot period. We have added a new figure (Figure S7) in the supplementary information to show the variability (i.e. average ± one standard deviation) of these items. The caption of Figure 2 has been modified to direct the reader to Figure S7 if they are interested in the variability of these measurements.

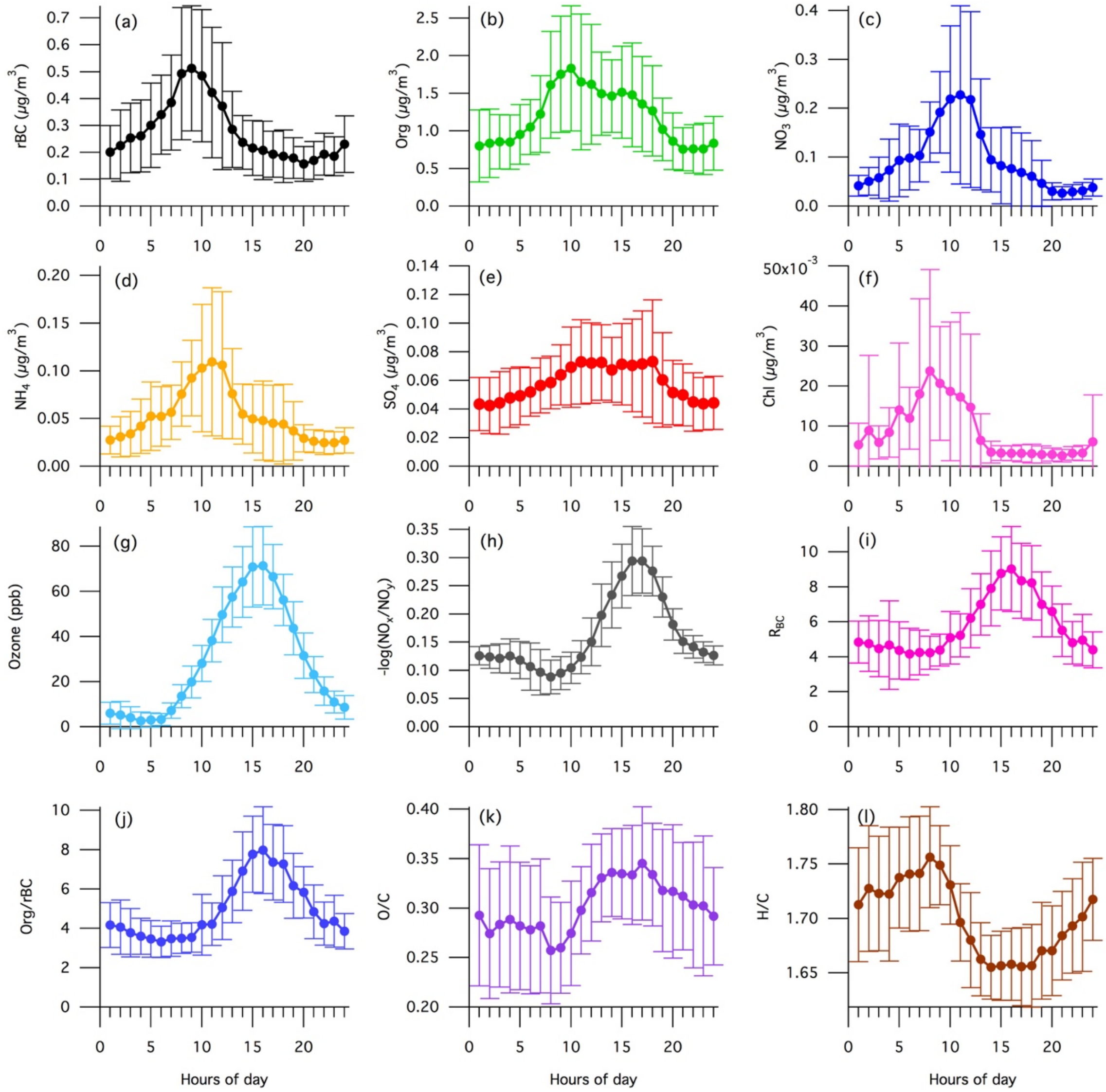

Figure S7: Diurnal cycles of (a) rBC, NR-PM$_{rBC}$ components, including (b) Organics, (c) nitrate, (d) ammonium, (e) sulfate and (f) chloride, (g) ozone, (h) -log(NO$_x$/NO$_y$), (i) R$_{BC}$, (j) Org/rBC ratio, (k) O/C and (l) H/C of organic coating. The data points represent average values and the error bars represent one standard deviation.

Line 26-31, page 5: During the daytime from July 21to 22, mass loadings of rBC and nitrate peaked in the afternoon on July 21 and in the morning on July 22 while the NOx mixing ratios kept at relatively low levels. Does this indicate that other sources of rBC existed? Should the data on these two days be excluded from the calculation? Also, the poor correlation between NOx and nitrate on these days may indicate formation mechanisms of particulate NH4NO3 other than the OH radicals oxidation of NO2.

Response:

Thanks for addressing this interesting point. rBC can be emitted from any combustion sources but we did not identify combustion emissions (such as biomass burning) other than traffic from the PMF analysis of both HR-ToF-AMS and SP-AMS measurements. Furthermore, SP-AMS data is not available on the morning of July 21 so that we cannot comment whether the nitrate concentrations would have peaked in the morning on this day. We have tried to exclude that short period of time to calculate the diurnal cycles of individual species. The changes in diurnal patterns and concentrations are only minimal and thus we decide to keep the original period for all the subsequent calculation in this work. We agree that the elevated NH_4NO_3 concentrations within that short period of time might be due to regional transport and/or produced through mechanisms other than OH radical oxidation of NO_2. Since this paper aims to present the general observations/patterns of aerosol species within the entire hot period, we decided to not discuss this individual event in the revised manuscript in order to avoid any potential confusion to readers.

Line 37-39, page 5: Although sulfate followed the diurnal patterns of nitrate in the morning, it does not really mean its significant formation from photochemistry. Is it possible that regional transportation contributed to this pattern? Is there any other evidence such as the pattern of the precursor gas SO2 to draw this statement? Figure 1 shows that there are quite some changes in wind directions/speed during the hot periods.

Response:

Reviewer 1 also points out this possibility. The sentence has been revised as shown below to address the possibility of regional transport of sulfate during the day.

Page 6: “Sulfate remained in low concentrations with a relatively modest pattern (see also Figure 5d) potentially caused by the transport of regional pollution into the area during the day”

Page 6. The authors have indicated that Cx+ signals can be derived from standard rBC. However, in the PMF analysis of the NR-PMrBC, Cx+ were used to identify an rBC rich factor. I am somewhat confused here. Are data on Figure 3 and discussions on Page 6 (first paragraph) are for the whole particle or the coating? If they are just for the coating, why do these Cx+ exist and how would we know if they are not from rBC?

Response:

C_x^+ ions (from rBC) were included in the PMF analysis to identify potential mass contributions of rBC to each PMF factor (i.e., each PMF factor consists of both rBC and OA components). This approach has been used in our previous studies (Willis et al., 2016, and Lee et al., 2015, 2016). Signals of C_x^+ fragments can be used to calculate rBC mass (or mass fraction) in each PMF factor whereas other organic fragments represent different types of organic coating. To avoid potential confusion here, we modify a sentence in the experimental section as following:

Page 4: "Positive matrix factorization (PMF) was performed to investigate the potential sources and characteristics of rBC and organic aerosol components. Signals of C_x^+ fragments from rBC were included in the PMF analysis so that mass fraction of rBC and organic components can be calculated for each PMF factor (Lee et al., 2015; 2016;Willis et al., 2016)."

Line 20-30, page 6. What is the major source of OOA-2? It does not seem to be the result of further reactions of OOA-1. The authors also discard the possibility of regional transport although it was mentioned in the conclusion later.

Response:

While OOA-2 was likely due to local photochemistry, the possibility of regional transport of OOA-2 has been pointed out in the discussion as shown below:

Page 6: "OOA-2 represented a more oxygenated fraction of SOA coating (O/C = 0.62) with the maximum mass loadings observed at ~15:00-16:00 and its diurnal pattern matched well with Org/rBC ratios (Figures 2b and 3h). The diurnal pattern of OOA-2 indicates the importance of local photochemistry for OOA-2 production in the afternoon but the contribution of regional transport to OOA-2 cannot be completely ruled out. Given that rBC accounted for only 0.5 wt% of OOA-2 (i.e. much lower than other PMF factors), OOA-2 could represent SOA materials generated through local photochemistry and/or formed regionally under conditions with relatively low rBC particle concentrations."

Line 33, Line 6. It is a bit awkward to me that RBC is called "thickness", given that it is a mass ratio.

Response:

The term "coating thickness" has been removed from the heading of Section 3.2.

Line 6-7, page 7: The term POA may confuse the readers that COA is also included.

Response:

The term “POA” has been changed to “traffic-related POA” to avoid confusion.

Line 4-11, page 8: As shown in Figure S6, COA exhibited two peaks, one was around 17:00-18:00 similar to that of VOOA and the other larger peak was at midnight. This trend is largely different from typical diurnal patterns of COA that show a strong peak during dinner time. Also, large fractions of oxidized fragments were observed for *m/z*28, 42 and 55 in COA mass spectra. Could COA be already oxidized and not primary in origin?

Response:

The updated results of PMF analysis is shown in Figure S6 in SI. Signals of organic fragments at m/z 30 and 46 were removed from the PMF input due to the significant interferences of nitrate fragments to these organic fragments (Chen et al., submitted). Figure S6b shows the updated mass spectrum of COA, which has O/C and H/C ratios of 0.12 and 1.83 respectively. Even though COA peaked at around 18:00-19:00, the updated values of O/C and H/C ratios suggests the primary nature of the observed COA. The mass spectral characteristics of COA (i.e. high m/z 55/57 and m/z 41/43 ratios and relatively low contributions of oxygenated fragments to total organic) are also consistent to relatively fresh COA observed from previous studies (e.g., Mohr et al., 2012, Kaltsonoudis et al., 2017). The detail of PMF factors determined from NR-PM has been discussed in our companion study (Chen et al., submitted), and thus is not the focus of this work. However, it is worth noting that high levels of COA factor over mid-night is observed previously at a rural site (Dall’Osto et al., 2015), suggesting that the nature and origins of COA are complex and can include more than food cooking.

Line 15, page 8. Can organic sulfur compounds be formed in relation to VOOA? Huang et al. (2015) estimated OS lower bounds based on AMS measurements in HK.

Response:

Formation of organic sulfur compounds is certainly an interesting topic in aerosol chemistry. Concentrations of organic sulfur compounds in NR-PM was not correlated well with VOOA in this field study, and this information has been reported in our companion study (Chen et al., submitted). The results of comprehensive HR-ToF-AMS data analysis can also be found in that paper as well.

At times, I am confused what exactly rBC means. Is it the refractory BC without OA or including the OA (coating) on the BC? For example, line 8 on page 7, it says “OOA-1 contributed up to ~60 wt% of rBC mass…” This may be related to my earlier question on the nature of Cx+. On the other hand, terminology like rBC rich OA factor seems to imply a different definition of rBC. Figure 4 also uses "total rBC".

Response:

rBC is refractory black carbon without OA. This technical term has been used to describe black carbon measured by SP-AMS and SP2. As mentioned in our previous response, C_x^+ ions (from rBC) were included in PMF analysis to identify potential mass contributions of rBC to each PMF factor (i.e., each PMF factor consists of both rBC and OA components). This approach has been used in our previous field studies (Willis et al., 2016, and Lee et al., 2015, 2016). Signals of C_x^+ fragments can be used to calculate rBC mass (or mass fraction) for each PMF factor whereas other organic fragments represent different types of organic coating.

For example, rBC accounts for ~14 wt% and ~44 wt% of HOA-rich and rBC-rich factors, respectively (Page 6). In other words, OA accounts for ~86 wt% and 56 wt% of HOA-rich and rBC-rich factors, respectively. Similarly, based on the mass fraction of rBC determined in each PMF factor, the contribution of each PMF factor to total rBC concentrations can be calculated as shown in Figure 4d.

A conclusion is that the OOA in coatings of rBC are less oxygenated than those in VOOA. Just a speculation, would it be possible that the OOA in rBC condensed onto HOA coated rBC which promote partitioning of less oxygenated species while VOOA condensed on more hydrophilic particles?

Response:

This speculation is possible. However, as pointed out by Reviewer 1, we cannot provide direct evidence of a mechanistic preference for material to condense onto certain surfaces, we have changed our tone in the revised version to highlight this possibility for future research.

Page 10: "There may be also a mechanistic preference for material to condense onto certain surfaces because of their chemical nature (e.g., hydrophobic coating (e.g. HOA and soot surface functionality) but more research efforts are required to explore this possibility."

Technical comments:

Line 18, page 1: "missions" should be "emissions".

Response: The typo has been corrected.

Reference:

Aiken, A. C., DeCarlo, P. F., and Jimenez, J. L.: Elemental Analysis of Organic Species with Electron Ionization High-Resolution Mass Spectrometry, Analytical Chemistry, 79, 8350-8358, 10.1021/ac071150w, 2007.

Aiken, A. C., DeCarlo, P. F., Kroll, J. H., Worsnop, D. R., Huffman, J. A., Docherty, K. S., Ulbrich, I. M., Mohr, C., Kimmel, J. R., Sueper, D., Sun, Y., Zhang, Q., Trimborn, A., Northway, M., Ziemann, P. J., Canagaratna, M. R., Onasch, T. B., Alfarra, M. R., Prevot, A. S. H., Dommen, J., Duplissy, J., Metzger, A., Baltensperger, U., and Jimenez, J. L.: O/C and OM/OC Ratios of Primary, Secondary, and Ambient Organic Aerosols with High-Resolution Time-of-Flight Aerosol Mass Spectrometry, Environ. Sci. Technol., 42, 4478-4485, 10.1021/es703009q, 2008.

References:

Chen, C.-L., Chen, S., Russell, L. M., Liu, J., Price, D. J., Betha, R., Sanchez, K. J., Lee A. K. Y., Collier, S. C., Zhang, Q., Kumar, A., Kleeman, M., Zhang, X., and Cappa, C. D.: Organic aerosol particle chemical properties associated with residential burning and fog in wintertime San Joaquin Valley (Fresno) and with vehicle and firework emissions in summertime South Coast Air Basin (Fontana), submitted.

Dall'Osto, M., Paglione, M., Decesari, S., Facchini, M. C., O'Dowd, C., Plass-Duellmer, C., and Harrison, R. M.: On the Origin of AMS "Cooking Organic Aerosol" at a Rural Site, Environmental Science & Technology, 49 (24), 13964-13972, 2015.

Kaltsonoudis, C., Kostenidou, E., Louvaris, E., Psichoudaki, M., Tsiligiannis, E., Florou, K., Liangou, A., and Pandis, S. N.: Characterization of fresh and aged organic aerosol emissions from meat charbroiling, Atmos. Chem. Phys., 17, 7143-7155, https://doi.org/10.5194/acp-17-7143-2017, 2017.

Lee, A. K. Y., Willis, M. D., Healy, R. M., Onasch, T. B., and Abbatt, J. P. D.: Mixing state of carbonaceous aerosol in an urban environment: single particle characterization using the soot particle aerosol mass spectrometer (SP-AMS), Atmospheric Chemistry and Physics, 15, 1823-1841, 10.5194/acp-15-1823-2015, 2015.

Lee, A. K. Y., Willis, M. D., Healy, R. M., Wang, J. M., Jeong, C. H., Wenger, J. C., Evans, G. J., and Abbatt, J. P. D.: Single-particle characterization of biomass burning organic aerosol (BBOA): evidence for non-uniform mixing of high molecular weight organics and potassium, Atmospheric Chemistry and Physics, 16, 5561-5572, 10.5194/acp-16-5561-2016, 2016.

Mohr, C., Huffman, J. A., Cubison, M. J., Aiken, A. C., Docherty, K. S., Kimmel, J. R., Ulbrich, I. M., Hannigan, M., and Jimenez, J. L.: Characterization of Primary Organic Aerosol Emissions from Meat Cooking, Trash Burning, and Motor Vehicles with High-Resolution Aerosol Mass Spectrometry and Comparison with Ambient and Chamber Observations, Environmental Science & Technology, 43 (7), 2443-2449, 2009.

Willis, M. D., Lee, A. K. Y., Onasch, T. B., Fortner, E. C., Williams, L. R., Lambe, A. T., Worsnop, D. R., and Abbatt, J. P. D.: Collection efficiency of the soot-particle aerosol mass spectrometer (SP-AMS) for internally mixed particulate black carbon, Atmospheric Measurement Techniques, 7, 4507-4516, 10.5194/amt-7-4507-2014, 2014.

Willis, M. D., Healy, R. M., Riemer, N., West, M., Wang, J. M., Jeong, C. H., Wenger, J. C., Evans, G. J., Abbatt, J. P. D., and Lee, A. K. Y.: Quantification of black carbon mixing state from traffic: implications for aerosol optical properties, Atmospheric Chemistry and Physics, 16, 4693-4706, 10.5194/acp-16-4693-2016, 2016.

Formation of secondary organic aerosol coating on black carbon particles near vehicular emissions

Alex K. Y. Lee[1], Chia-Li Chen[2], Jun Liu[2], Derek J. Price[2], Raghu Betha[2], Lynn M. Russell[2], Xiaolu Zhang[3, #] and Christopher D. Cappa[3]

[1]Department of Civil and Environmental Engineering, National University of Singapore, Singapore
[2]Scripps Institution of Oceanography, University of California, San Diego, USA
[3]Department of Civil and Environmental Engineering, University of California, Davis, USA
[#]Now at: Crocker Nuclear Laboratory, University of California, Davis, USA

Correspondence to: Alex K. Y. Lee (ceelkya@nus.edu.sg)

Abstract. Black carbon (BC) emitted from incomplete combustion can result in significant impacts on air quality and climate. Understanding the mixing state of ambient BC and the chemical characteristics of its associated coatings are particularly important to evaluate BC fate and environmental impacts. In this study, we investigate the formation of organic coatings on BC particles in an urban environment (Fontana, California) under hot and dry conditions using a Soot-Particle Aerosol Mass Spectrometer (SP-AMS). The SP-AMS was operated in a configuration that can detect refractory BC (rBC) particles and their coatings exclusively. Using the –log(NO_x/NO_y) ratio as a proxy for photochemical age of air masses, substantial formation of secondary organic aerosol (SOA) coatings on rBC particles was observed due to active photochemistry in the afternoon, whereas primary organic aerosol (POA) components were strongly associated with rBC from fresh vehicular emissions in the morning rush hours. There is also evidence that cooking related organic aerosols were externally mixed from rBC. Positive matrix factorization and elemental analysis illustrate that most of the observed SOA coatings were freshly formed, providing an opportunity to examine SOA coating formation on rBC near vehicular emissions. Approximately 7-20 wt% of secondary organic and inorganic species were estimated to be internally mixed with rBC on average, implying that rBC is unlikely the major condensation sinks of SOA in this study. Comparison of our results to a co-located standard high-resolution time-of-flight aerosol mass spectrometer (HR-ToF-AMS) measurement suggests that at least a portion of SOA materials condensed on rBC surface were chemically different from oxygenated organic aerosol (OOA) particles that were externally mixed with rBC, although they could be both generated from local photochemistry.

Deleted: Diurnal cycles of oxygenated organic aerosol (OOA) observed by a co-located standard high-resolution time-of-flight aerosol mass spectrometer (HR-ToF-MS) correlated well with that of SOA coatings on rBC, but their mass spectral characteristics were different from each other. Our results suggest that at least a portion of SOA materials condensed on rBC surface were chemically different from OOA particles that were externally mixed with rBC, although they are both generated from local photochemistry.

1. Introduction

Black carbon (BC) emitted from incomplete combustion of fossil fuel and biomass has profound impacts on air quality and climate. BC is the dominant absorber of visible solar radiation in the atmosphere, introducing significant contributions to positive radiative forcing on both regional and global scales (Ramanathan and Carmichael, 2008;Bond et al., 2013). Organic coatings can be formed on BC through condensation and/or coagulation of co-emitted primary organic aerosol (POA) and secondary organic aerosol (SOA) produced via photochemical processing. The hydrophilic nature of SOA coating has been shown to modify hygroscopicity of ambient BC for cloud droplet activation (Kuwata et al., 2009;McMeeking et al., 2011;Laborde et al., 2013;Liu et al., 2013). Increasing coating thickness may enhance light absorption of BC due to a "lensing effect" depending on the degree of particle aging (Jacobson, 2001;Cappa et al., 2012;Peng et al., 2016;Liu et al., 2017), and alter BC morphology from highly fractal to compact structures and thus their aerodynamic properties (Moffet and Prather, 2009;Schnitzler et al., 2014;Guo et al., 2016;Peng et al., 2016). Understanding the mixing state of ambient BC and the chemical characteristics of its associated coatings is therefore particularly important to evaluate their fate and environmental impacts.

In typical urban environments, traffic emission is one of the major sources of BC particles. A complex mixture of gas-phase organic compounds with a wide range of volatility and molecular structure are co-emitted with BC from vehicles, contributing prominently to the urban SOA burden (Gentner et al., 2017 and references therein). Although it is not straightforward to identify the role of individual SOA precursors, previous studies have shown that organic coating thickness of BC particles and their degree of oxygenation increased with photochemical age or oxidant levels in the atmosphere (Cappa et al., 2012;Liu et al., 2015;Wang et al., 2017). Of particular concern is the timescale that is required for sufficient SOA condensation to modify the physical, chemical and optical properties of BC near emission sources. Peng et al. (2016) recently performed on-site chamber experiments to examine coating formation on size-selected BC seeds using SOA precursors from particle-free ambient air, demonstrating that only a few hours of photochemical aging can lead to complete particle morphology modification and light absorption enhancement of BC in polluted urban regions. Moffet and Prather (2009) also provided field evidence that fresh BC can quickly evolve in terms of particle morphology in a photochemically active urban environment by developing coatings of secondary species over a timescale of several hours, highlighting the importance of local SOA chemistry on BC aging mechanisms.

While most previous studies focused on determining potential effects of SOA coatings to the BC properties, there is still a lack of laboratory and field investigations to examine effectiveness and selectivity of BC seed particles for condensation of SOA materials especially in the presence of other existing seed particles. Recent field observations reported that SOA condensed on BC only accounted for 35% and 41% of total SOA mass near traffic emission sources and in a polluted offshore environment, respectively (Massoli et al., 2012;2015). Metcalf et al. (2013) conducted a series of smog chamber experiments to investigate photooxidation of naphthalene and α-pinene in the presence of both BC and ammonium sulfate seed particles with comparable surface area of each particle type. Although their observations indicated that the use of BC as a seed is not expected to alter the overall basic chemistry of SOA formation, whether the SOA condensed on BC particles is chemically different from those condensed on ammonium sulfate particles or formed through homogeneous nucleation remains unclear.

Real-time and mass-based chemical compositions of organic coatings on ambient BC particles were seldom reported until the recent development of an Aerodyne Soot-Particle Aerosol Mass Spectrometer (SP-AMS) (Cappa et al., 2012;Massoli et al., 2012;2015;Onasch et al., 2012;Liu et al., 2015;Lee et al., 2016;Willis et al., 2016). In this study, we investigate formation of organic coatings on BC particles by deploying a SP-AMS in Fontana, California, which is located in the broader South Coast Air Basin and includes the greater Los Angeles area. The sampling site was located in an urban environment with strong influences of vehicular emissions. The SP-AMS was operated in a configuration that can detect refractory BC (rBC) and their coating materials exclusively. The term of rBC is operationally defined (Onasch et al., 2012) and will be used throughout the rest of this paper. The repeated diurnal patterns of inorganic species, POA and SOA that are internally mixed with rBC reported here provides a unique opportunity to investigate the chemical characteristics and formation of POA and SOA coatings on rBC particles near traffic emissions. A co-located Aerodyne High resolution Time-of-Flight Aerosol Mass Spectrometer (HR-ToF-AMS) was operated simultaneously to quantify the total amounts of non-refractory organic and inorganic species in PM_1 (Chen et al., 2017). The results provide insights into the effectiveness of rBC particles as a condensation sink of fresh SOA near traffic emissions and the chemical characteristics of SOA coatings compared to SOA that were externally mixed with rBC.

2. Experiment

2.1 Sampling location and instrumentations

The sampling site in Fontana, managed by South Coast Air Quality Management District (SCAQM), was located behind the fire station at 14360 Arrow Highway (34.100 N, 117.490 W). Surrounded by the I-15 freeway to the west (4.3 km), I-10 freeway to the east (3.9 km), and an auto speedway to the south, the sampling site was strongly influenced by vehicular emissions, as well as the broader urban plume. Aerosol particle instruments housed in a sampling van with a custom isokinetic inlet were deployed. Air pulled through the inlet was dried using diffusion driers and subsequently distributed to different real-time particle instruments. This study focuses on the results from a soot-particle aerosol mass spectrometer (SP-AMS, Aerodyne Research) that was configured to detect rBC-containing particles and their coating materials exclusively (See Sections 2.2 and 2.3 for the descriptions of SP-AMS and the calibration approach, respectively). The details of other particle instruments, including a high-resolution time-of-flight aerosol mass spectrometer (HR-ToF-AMS, Aerodyne Research), a single-particle soot photometer (SP2, Droplet Measurement Technologies), and a scanning electrical mobility spectrometer (SEMS, Brechtel) have been reported in Chen et al. (2017) and Betha et al. (2017). Two nitrogen oxide analyzers (Model 42i and 42i NO_y, Thermo Fisher Scientific) were used to measure mixing ratios of NO_x and NO_y for determining photochemical age (PCA) of air masses. The heated molybdenum converter in the 42i nitrogen oxide analyzer was replaced by an UV-LED photolytic NO_2 converter (Air Quality Design) for NO_x measurement. Hourly average ozone data was obtained from the co-located SCAQM air monitoring station.

Measurements were performed from 5 to 28 July 2015 with ambient temperature varying from 14.9 to 35.9 °C. Companion studies have shown that aerosol compositions were strongly influenced by fireworks from 4 to 8 July 2015 (Chen et al., 2017; Betha et al., 2017). There were few clouds and little precipitation with the exception of a short storm with high rainfall and winds on 18–19 July (two-day precipitation = 3.6 cm and maximum wind speed = 10 ms^{-1}). Sampling days with the maximum daily temperature above 30 °C (11–17 and 20–28 July) and lower than 27 °C (9–10 July) were classified as “hot” and “cooler” days, respectively (Chen et al., 2017). The identified hot days were dry with the average hourly relative humidity (RH) varied between 30 and 50% during the daytime. The Hybrid Single-Particle Lagrangian Integrated Trajectory (HYSPLIT) model with input from NOAA Air Resource Laboratory Archived Eta Data Assimilation System was used (http://www.arl.noaa.gov/HYSPLIT_info.php) to evaluate whether particular upwind source regions affected the aerosol measured at the sampling site. Air mass back trajectories were consistently westerly from the coast within the entire sampling period except for the storm days (Chen et al., 2017). Classification of sampling periods based on meteorological conditions and pollutant characteristics is shown in Figure 1.

2.2 Soot particle aerosol mass spectrometer (SP-AMS)

The working principle of SP-AMS has been reported in detail previously (Onasch et al., 2012). In brief, rBC-containing particles are vaporized at ~4000 K by a 1064 nm continuous wave intracavity infrared laser similar to that of the SP2 instrument (Onasch et al., 2012). The resulting vapour is ionized via 70 eV electron impact and then detected by a high-resolution time-of-flight mass spectrometer operated in V-mode, which provides a mass resolving power of ~2000 at m/z 28 (DeCarlo et al., 2006;Canagaratna et al., 2007). Note that BC particles detected by SP-AMS are operationally defined as refractory black carbon (rBC). A resistively heated tungsten vaporizer was removed from our instrument so that only rBC and its coating materials were detected (Massoli et al., 2012;2015;Lee et al., 2016;Willis et al., 2016). An efficient particle time-of-flight system (ePToF, multi-slit chopper with 50% aerosol throughput) was used for measuring aerosol size distributions. The SP-

AMS was operated alternating between ensemble mode (i.e., 1-min average of bulk mass spectrum and PToF size distribution) and event trigger mode (i.e., single particle mass spectrum with PToF size).

The SP-AMS was operated from 6 to 28 July 2015 and only the ensemble measurements are reported in this paper. The ensemble data were processed using the AMS data analysis software (Squirrel, version 1.56D for unit mass resolution data and Pika, version 1.15D for high resolution data from http://cires1.colorado.edu/jimenez-group/ToFAMSResources/ToFSoftware/) with the corrected air fragment column of the standard fragmentation table (Allan et al., 2004;DeCarlo et al., 2006). In particular, the average contribution of gas-phase CO_2 to CO_2^+ organic fragment in particle phase was determined (i.e., CO_2–to-N_2 ratio) based on the measurements of particle-free ambient air (i.e., at least 10 min per day) throughout the sampling period. Positive matrix factorization (PMF) was performed to investigate the potential sources and characteristics of rBC and organic aerosol components. Signals of C_x^+ fragments from rBC were included in the PMF analysis so that mass fraction of rBC and organic components can be calculated for each PMF factor (Lee et al., 2015; 2016;Willis et al., 2016). The bilinear model was solved using the PMF2 algorithm in robust mode (Paatero and Tapper, 1994) and a final solution was selected using the PMF Evaluation Tool (PET) version 2.06 according to the method described previously (Ulbrich et al., 2009;Zhang et al., 2011). A four-factor solution, including two POA factors from traffic emissions and two SOA factors due to local photochemistry, was selected by examining the solutions for up to eight PMF factors (see supplementary information). Elemental analysis (i.e., oxygen- and hydrogen-to-carbon ratios, O/C and H/C) was performed based on the improved ambient method (Canagaratna et al., 2015a).

2.3 SP-AMS calibration

A water suspension of Regal Black (Regal 400R Pigment Black, Cabot Corp., a calibration standard recommended by Onasch et al., 2012), was atomized using a constant output atomizer (TSI Inc., Model 3076) for generating standard rBC particles. Dried 300 nm Regal Black particles were used to determine mass-based ionization efficiency of rBC (mIE_{rBC}). Signals for Regal Black particles were quantified by the sum of carbon ion clusters (C_x^+, i.e. C_1^+-C_9^+) using high-resolution mass spectral data. The average C_1^+ to C_3^+ ratio of 0.478 obtained from Regal Black calibration was used to correct the interference in C_1^+ from non-refractory organics in ambient aerosol. The product of material density and the Jayne shape factor (also defined as effective density, ρ_{eff}) of the dried 300 nm Regal Black particles was 0.86±0.02 g/cm^3, which can be derived from the ratio of the vacuum aerodynamic diameter (d_{va}) measured by the SP-AMS to the mobility diameter (d_m) selected by a differential mobility analyzer (DMA) as follow:

$$\rho_{eff} = \rho_m S = (d_{va} / d_m)\, \rho_0 \qquad \text{(Eq.1)}$$

where ρ_m and S are the material density and Jayne shape factor, respectively, and ρ_0 is the unit density (DeCarlo et al., 2004). The average effective density of 0.86 and d_m were used to further calculate the mass of individual dried 300 nm Regal Black particles (DeCarlo et al., 2004) which was approximately 12.2 fg. The average mIE_{rBC} value was 255±50 ions/pg of Regal Black particle based on three independent calibrations performed throughout the study.

Direct calibration of the ionization efficiency for nitrate (IE_{NO3}) is not possible without the tungsten vaporizer. Before removal of the tungsten vaporizer from the SP-AMS, dried 300 nm pure ammonium nitrate (NH_4NO_3) and Regal Black particles were generated for determining mass-based ionization efficiency of nitrate (mIE_{NO3}) and mIE_{rBC}, respectively. Note that the mIE_{NO3} was determined without operating the laser vaporizer. The relative ionization of rBC ($RIE_{rBC} = mIE_{rBC}/mIE_{NO3}$) was 0.26. Assuming that RIE_{rBC} remains unchanged after removing the tungsten vaporizer, mIE_{NO3} and IE_{NO3} were calculated based on measured values of mIE$_{rBC}$. The calculated IE$_{NO3}$ was then used with recommended RIE values (Jimenez et al. (2003), i.e., nitrate = 1.1, sulfate = 1.2, chloride = 1.3, organics = 1.4 and ammonium = 4) to quantify non-refractory aerosol species associated with rBC (referred to as NR-PM$_{rBC}$). Note that our previous studies have shown that this calibration approach likely yields the calculated IE$_{NO3}$ values as a lower limit, leading to over quantification of the NR-PM$_{rBC}$ mass loadings in ambient aerosol (Willis et al., 2014;Lee et al., 2015).

The collection efficiency (CE) for rBC particles that is governed by the degree of overlap between particle and laser beams was determined using beam width probe (BWP) measurements described previously (Willis et al., 2014). Ambient rBC-containing particles had an average beam width (σ) = 0.45±0.04 mm based on three sets of BWP measurements performed throughout the study. The measured particle beam width suggests a condition of incomplete beam overlap, arising from non-spherical rBC particles, and hence a CE of 0.6 was applied for absolute quantification of rBC and NR-PM$_{rBC}$ (Willis et al., 2014). All BWP measurements were performed around the morning rush hours. Fresh rBC-containing particles from vehicular emissions in the morning had thinner coatings compared to those rBC-containing particles observed in the afternoon that were more photochemically aged (see discussion in Section 3). It has been demonstrated that CE for rBC particles increases (or rBC particle beam width decreases) with coating thickness (Willis et al., 2014). The applied CE may be therefore less relevant for the time with high ambient SOA loading (i.e., high NR-PM$_{rBC}$/rBC mass ratio, or R$_{BC}$), leading to over quantification of the SOA components in NR-PM$_{rBC}$ by at most 40% due to this uncertainty. Furthermore, a wider particle beam than the laser beam implies that some rBC-containing particles may undergo incomplete vaporization at the edges of the laser vaporizer, which would in turn bias the measurement towards the coatings rather than the rBC cores (see unpublished data from, http://cires.colorado.edu/jimenezgroup/UsrMtgs/UsersMtg16/JDASPAMSfocusing.pdf). Since the CE of 0.6 was primarily determined for rBC, this phenomenon may further increase the degree of over quantification of NR-PM$_{rBC}$. Overall, the values of NR-PM$_{rBC}$ reported in this work likely represent their upper limits.

Deleted: The applied CE may be therefore less relevant for the time with high ambient SOA loading (i.e., high NR-PM$_{rBC}$/rBC mass ratio, or R$_{BC}$), leading to over quantification of the SOA components in NR-PM$_{rBC}$ by at most 40% due to this uncertainty.. Nevertheless, the CE applied does not impact calculations of R$_{BC}$ in the rBC-containing particles. unpublished data from, Since the CE of 0.6 was primary determined for rBC, this phenomena may further increase the degree of over quantification of NR-PM$_{rBC}$. Overall, the values of NR-PM$_{rBC}$ reported in this work likely represent their upper limits.

3. Results and Discussion

Figure 1 shows the time series of meteorological data (temperature, relative humidity (RH), wind direction and wind speed), mixing ratios of ozone and NO$_x$, NO$_x$/NO$_y$ ratio, and chemical compositions of rBC-containing particles (i.e., rBC and NR-PM$_{rBC}$) from 5 to 28 July 2015. The whole sampling period can be divided into four categories as previously reported (Chen et al., 2017; Betha et al., 2017). In brief, fireworks had strong impacts on aerosol compositions from 5 to 8 July, and significant enhancements of inorganic aerosol components were observed in rBC-containing particles (Figure 1f). After the firework period, mass loadings of rBC-containing particles remained low from 9 to 10 July without clear diurnal patterns (indicated as cooler days in Figure 1). A storm cleaned up the atmosphere from 18 to 19 July, leading to very low levels of all aerosol components within the two days. The SP-AMS was under maintenance from 20 July 18:00 to 21 July 12:00. The weather was relatively hot and dry for the rest of sampling days (indicated as hot days in Figure 1). Repeated diurnal patterns of Org/rBC ratio (or R$_{BC}$) with peak values in the afternoon were observed over the hot period (Figure 1e), indicating a unique opportunity to examine POA and SOA formation on rBC near vehicular emissions via daytime chemistry. The observations during the hot period will be the focus of the following discussion.

3.1 Chemical characteristics of rBC coating materials (NR-PM$_{rBC}$)

Figure 2a shows the average diurnal cycles of rBC and NR-PM$_{rBC}$ during the hot period. Mass loadings of rBC increased continuously in the morning rush hours and peaked at ~8:00–9:00, and they were strongly correlated with the NO$_x$ mixing ratio (r = 0.82), consistent with local traffic emissions as a major source (Figure 1d). Boundary layer break up led to the decrease of rBC and NO_x concentrations (i.e., dilution as air from residual layer mixed down to the surface). These diurnal patterns indicate that there were minimal influences of other combustion sources such as biomass burning and industrial emissions to the observed rBC concentrations. Nitrate and ammonium concentrations correlated well with each other (r = 0.97). Their mass loadings increased slowly over the night and reached the maximum levels at ~10:00–11:00 in the morning (Figure 2a). While NO_2 reacts with ozone to generate N_2O_5 at night, OH radicals oxidation of NO_2 during daytime produce nitric acid that can be neutralized by ammonia, forming particulate NH_4NO_3. A recent tunnel study has observed such NH_4NO_3 formation chemistry in aged traffic emissions (Tkacik et al., 2014). The decrease of particulate nitrate and ammonium (i.e., NH_4NO_3) concentrations could be the combined effects of boundary layer break up and evaporative loss at the increasing temperature during the day. Sulfate remained in low concentrations with a relatively modest pattern (see also Figure 5d) potentially caused by the transport of regional pollution into the area during the day. Chloride was also associated with traffic (see also Figure 5e) and was likely due to condensation of HCl vapor that was subsequently neutralized by ammonia (i.e., formation of NH_4Cl).

Deleted: Although sulfate remained in relatively low concentrations in both day and night time, it followed the diurnal patterns of nitrate in the morning (see also Figure 5d), indicating significant contributions from local secondary aerosol formation chemistry.

Organic aerosol (OA) was the dominant component of NR-PM_{rBC} during the hot period as illustrated in Figure 2a. Mass loadings of organic coating increased with rBC concentrations in the morning rush hours. PMF results show that two primary emission factors, referred to as hydrocarbon-like OA-rich (HOA-rich) and rBC-rich factors hereafter, were the major contributors to the total OA mass during the morning rush hours (Figure 3e and f). The mass concentration of the rBC-rich factor was slightly lower than the HOA-rich factor. Mass spectra of HOA- and rBC-rich factors indicate that rBC accounted for 14.2 and 44.4 wt% of the two primary aerosol factors, respectively. The fragmentation pattern of rBC was similar to those previously reported in urban environments near traffic emissions and engine exhausts (Massoli et al., 2012;Lee et al., 2015;Enroth et al., 2016;Willis et al., 2016;Saarikoski et al., 2017). With the support of single particle measurement, Willis et al. (2016) also separated traffic-related OA into HOA- and rBC-rich factors in the roadside environment using a SP-AMS with a tungsten vaporizer being removed and estimated that approximately 90% of rBC mass emitted from vehicle resided in rBC-rich particles. By following the calculation procedure described in Willis et al. (2016), rBC-rich factor contributed about 82 wt% of the freshly emitted rBC from traffic. Note that rBC-rich particles were composed of more oxygenated organic fragments compared to the HOA-rich factor (Figure 3a and b), likely due to the presence of refractory ion fragments (i.e., CO^+ and CO_2^+) that originated from oxygenated functionalities on the soot surface and in the soot nanostructure (Corbin et al., 2014;Malmborg et al., 2017).

Using –log (NO_x/NO_y) as a proxy for PCA of air masses and Org/rBC ratio (or R_{BC}) as an indicator for SOA formation, production of fresh SOA coating materials on rBC particles was observed due to active photochemistry in the afternoon (Figure 2b). The secondary nature of organic coatings observed in the afternoon peak was supported by the diurnal cycles of O/C, H/C and average carbon oxidation state ($OS_c \approx 2O/C – H/C$, Kroll et al. (2011)) of total OA (Figure 2d). Higher values of O/C and OS_c were observed in the afternoon compared to in the morning rush hours, consistent with the expectation that the O/C ratio of SOA is greater than POA. The PMF analysis identified two types of oxygenated OA (OOA), referred to as OOA-1 and OOA-2 hereafter, both of which are likely SOA coatings. Mass spectra of both OOA factors were dominated by an oxygen-containing organic fragment at m/z 43 (i.e., $C_2H_3O^+$, Figure 3c and d), similar to those previously observed by Massoli et al. (2015). OOA-1 represented less oxygenated SOA components (O/C = 0.53) with 13.4 wt% of rBC content, and its concentration started increasing in the morning coincident with nitrate and ammonium (i.e., peaks at ~10:00-11:00, Figure 2a and 3g) and sustained at relatively constant levels until ~15:00–16:00. This suggests a possibility that OOA-1 represented a fresher portion of SOA coating materials generated by photochemistry of anthropogenic gas-phase precursors from vehicular emissions. OOA-2 represented a more oxygenated fraction of SOA coating (O/C = 0.62) with the maximum mass loadings observed at ~15:00-16:00 and its diurnal pattern matched well with Org/rBC ratios (Figures 2b and 3h). The diurnal pattern of

Deleted: Figure 2c

Deleted: OOA-2 represented more oxygenated fraction of SOA coating (O/C = 0.62) with the maximum mass loadings observed at ~15:00-16:00 and its diurnal pattern matched well with Org/rBC ratios (Figures 2b and 3h). OOA-1 represented less oxygenated SOA components (O/C = 0.53) and, in addition to the afternoon peak, OOA-1 increased in the late morning coincident with nitrate and ammonium (i.e., peaks at ~10:00-11:00, Figure 2a and 3g). This suggests a possibility that OOA-1 represented a fresher portion of SOA coating materials generated by photochemistry of anthropogenic gas-phase precursors from vehicular emissions.

OOA-2 indicates the importance of local photochemistry for OOA-2 production in the afternoon but the contribution of regional transport to OOA-2 cannot be completely ruled out. Given that rBC accounted for only 0.5 wt% of OOA-2 (i.e. much lower than other PMF factors), OOA-2 could represent SOA materials generated through local photochemistry and/or formed regionally under conditions with relatively low rBC particle concentrations.

3.2 Chemical characteristics of OA as a function of R_{BC}

Figure 4a illustrates that R_{BC} increased continuously as a function of –log (NO_x/NO_y) within the hot period. Assuming ambient daytime OH radical concentration was ~4 × 10^6 molecules cm^{-3} (Takegawa et al., 2006;Slowik et al., 2011) and the major NO_x loss product was HNO_3, the estimated PCA values (i.e., PCA ≈ $-\ln([NO_x]/[NO_y]) / k_{rxn}[OH]$) were about 5-7 h in the afternoon given that the rate constant between OH radicals and NO_x for HNO_3 formation (k_{rxn}) is equal to 7.9 × 10^{-12} cm^3 $molecules^{-1}$ s^{-1} (Brown et al., 1999;Cappa et al., 2012). Such estimation further supports our hypothesis that OOA-1 and OOA-2 were fresh SOA produced in the local atmosphere. Furthermore, OA components became more oxygenated as the PCA and R_{BC} increased (i.e., solid circles with the coloured scale of OS in Figure 4a). Figure 4c illustrates that ~85-90 wt% of total NR-PM_{rBC} was organic regardless of the values of R_{BC}. POA from traffic emissions (i.e., rBC- and HOA-rich factors) accounted for ~50–70 wt% of total NR-PM_{rBC} when R_{BC} is smaller than 4 whereas the contributions of SOA components (i.e., OOA-1 and OOA-2 factors) increased with R_{BC}, reaching a plateau at about 70–75% of total NR-PM_{rBC} when R_{BC} is larger than 8.

Deleted: ~90 wt%

Deleted: ~60–75 wt%

Figure 4b shows that R_{BC} decreased continuously with higher rBC loadings, highlighting the fact that most of the rBC mass observed within the hot period was associated with POA materials. Based on the mass fraction of rBC signals in the mass spectra of each PMF factor, it can be estimated that over 80 wt% of rBC mass was associated with traffic-related POA (i.e., about 60 and 20 wt% from rBC-rich and HOA-rich factors, respectively) when R_{BC} is smaller than 4 (Figure 4d). An increasing contribution of OOA factors to rBC mass was observed for particles with thicker OA coating. OOA-1 factor contributed up to ~60 wt% of rBC mass when R_{BC} is larger than 10 while OOA-2 factor was only a minor contributor to rBC mass for the whole range of R_{BC} values. The small contribution of OOA-2 particles to the rBC burden occurred despite the substantial contribution of OOA-2 to the total NR-PM_{rBC} mass. This is because rBC accounted for only 0.5 wt% of the OOA-2 factor, implying that such OOA materials co-existed with small rBC inclusions. Willis et al. (2014) reported that SP-AMS could accurately measure the mass fraction of rBC, at least down to 0.05 (5 wt%), in laboratory-generated organically coated Regal Black particles. Vaporization efficiency of an individual particle with a tiny rBC core diameter (e.g., < 5 wt%) and its uncertainties to mass quantification remain unclear (e.g., insufficient volatilization may lead to an underestimate of mass in the factor).

Deleted: POA

3.3 Comparisons of NR-PM_{rBC} and NR-PM components

To understand the mixing state of OA and rBC particles, the SP-AMS measurements (NR-PM_{rBC}) were compared to the co-located HR-ToF-AMS measurements (NR-PM) as presented in Figures 5 and 6. Mass loadings of secondary species in NR-PM_{rBC} were lower than their corresponding NR-PM components based on the CE and IE_{NO3} values used in this work, suggesting that significant fractions of secondary aerosol species were externally mixed with rBC. Specifically, diurnal cycles of nitrate, ammonium and chloride were strongly correlated ($r > 0.96$) between the two measurements but only about 8-20 wt% (or NR-PM_{rBC}/NR-PM = 0.08-0.2) of their masses were coated on rBC. The fraction of sulfate that was internally mixed with rBC was small, on average (NR-PM_{rBC}/NR-PM = 0.07). The relative abundance of HOA and OOA (i.e., comparing OA mass loadings in the morning and afternoon peaks in Figure 5a) suggests that a larger fraction of OOA was externally mixed with rBC compared to HOA from traffic emissions, discussed further below. In general, OOA and sulfate tend to be concentrated in the accumulation mode peaking between 400-600 nm in d_{va} (Zhang et al., 2011), and hence the above argument also explains the larger difference of OA and sulfate mass with d_{va} larger than 300 nm between the two measurements (Figure 5i).

Chen et al. (2017) identified four PMF factors, namely HOA, cooking OA (COA), nitrate-related OOA (NOOA) and very OOA (VOOA), to describe the potential sources of OA measured by the HR-ToF-AMS (Figure S6) in this field campaign. The HOA and COA factors are assumed primary and the NOOA and VOOA factors are assumed secondary in origin. First, HOA exhibited a strong peak in the morning rush hours, and its diurnal cycle and mass loading was very similar to the sum of rBC- and HOA-rich factors in terms of both shape and the absolute concentrations (Figures 5f). HOA accounted for 9 wt% of total OA in NR-PM. Figure 6 further demonstrates that the average ratio of NR-PM$_{rBC}$/NR-PM for HOA components (i.e., ([HOA-rich] + [rBC-rich]) / [HOA]) is about 1.32, implying that HOA materials were largely internally mixed with rBC but their concentrations in NR-PM$_{rBC}$ might be over quantified by 32% on average based on our CE correction and IE calibration approach. Note that the mass loadings of rBC contributing to the HOA-rich and rBC-rich factors (estimated from the C_n^+ ions) were subtracted in the calculation of NR-PM$_{rBC}$/NR-PM. Nevertheless, the presence of refractory oxygenated organic fragments in the mass spectra of the rBC-rich factor could introduce positive biases to such estimation. The average ratio drops to about 1.05 if the three major oxygenated organic fragments, including CO^+, CO_2^+ and $C_2H_3O^+$, are also excluded in the calculation. Using the same measurement approach and R_{BC}-dependent CE, Massoli et al. (2012; 2015) reported that 81 and 87 % of HOA were associated with rBC particles near vehicular emissions and in a polluted offshore environment.

Deleted: vehicle-related

Deleted: 11%

Deleted: 0.95

Deleted: Note that the mass loadings of rBC contributing to the HOA-rich and rBC-rich factors (estimated from the C_n^+ ions) were subtracted in the calculation of NR-PM$_{rBC}$/NR-PM. Nevertheless, the presence of refractory oxygenated organic fragments in the mass spectra of the rBC-rich factor could introduce positive biases to such estimation. The average ratio drops to about 0.85 if the three major oxygenated organic fragments, including CO^+, CO_2^+ and $C_2H_3O^+$, are also excluded in the calculation. Using the same measurement approach

COA was another POA that contributed to 14 wt% of total OA in NR-PM. However, COA was not identified in the PMF analysis of SP-AMS data. The comparison suggests that COA was unlikely co-emitted with rBC from modern kitchens, and the mixing of rBC and COA through particle coalescence was insignificant near the sampling location. Similar observations have been reported in previous studies in downtown Toronto. Willis et al. (2016) could not identify COA by measuring rBC-containing particles exclusively whereas Lee et al. (2015) could separate a COA factor from other OA components by deploying a SP-AMS equipped with dual vaporizers (i.e., laser and tungsten vaporizers). Comparing the results obtained from two different operational modes (i.e., switching laser vaporizer on and off), Lee et al. (2015) provided indirect evidence that COA was largely externally mixed with rBC in the urban atmosphere.

Deleted: 15 wt%

SOA was the most abundant OA component. VOOA and NOOA accounted for 60 and 17 wt% of total OA in NR-PM, respectively. Diurnal variations of NOOA were minimal, whereas VOOA mass concentrations increased continuously from ~8:00 and peaked at ~18:00 (Figures 5g and S6). Although PMF analysis identified two SOA factors for both AMS measurements, the total SOA concentrations were calculated to provide overall comparisons of SOA mass loadings in NR-PM and NR-PM$_{rBC}$ regardless their sources. Specifically, SOA$_{NR-PM}$ = NOOA + VOOA for HR-ToF-AMS and SOA$_{rBC}$ = OOA-1 and OOA-2 for SP-AMS. The average SOA$_{rBC}$/SOA$_{NR-PM}$ is equal to 0.2, indicating that approximately 20 wt% of OOA components were internally mixed with rBC on average during the hot period (Figure 6). It is worth noting that SOA$_{rBC}$ increased at a faster rate in the morning compared to SOA$_{NR-PM}$, suggesting that SOA$_{rBC}$ and SOA$_{NR-PM}$ could be produced or transported from different sources, at least to some extent. Furthermore, SOA$_{NR-PM}$ mass concentrations started dropping substantially at ~18:00-19:00, which was about 1-2 hours delay compared to SOA$_{rBC}$ (Figure 5g). This observable delay corresponded to the time of increasing sulfate levels in NR-PM, implying potential sources and formation pathways of VOOA (i.e., the major component of SOA$_{NR-PM}$ within that period) that might be related to the regional transport of aged particles. This possible explanation is consistent with the observation that VOOA represented more oxidized OOA materials (i.e. more aged) and that the strongest average wind speed was observed at around 18:00-19:00 (Figure 2c). Single particle measurements using the light scattering module of the HR-ToF-AMS also suggests internal mixing of sulfate and highly oxidized OOA materials in NR-PM (Chen et al., 2017). Nevertheless, VOOA could also be produced through local photochemistry as 1) it

Deleted: 64 and 10 wt%

was unlikely that all the locally formed SOA materials were condensed on rBC particles exclusively during the day and 2) the HR-ToF-AMS should be able to detect OOA-1 and OOA-2 materials as well. The relative contributions of local photochemistry and regional transport to the observed VOOA mass could not be separated by the PMF analysis possibly due to the chemical similarity of those SOA materials.

Deleted: Even though both OOA-2 and VOOA were formed through local photochemistry in the afternoon (Figure 5h), VOOA mass concentrations started dropping substantially at ~18:00, which was about 1-2 hours delay compared to the case of OOA-2. This observable delay corresponded to the time of increasing sulfate levels in NR-PM, implying additional sources and formation pathways of VOOA that might be related to the transport and formation chemistry of sulfate in NR-PM. VOOA might form in a downwind environment with less rBC loadings and advect to the site when the OOA-2 concentration dropped. The diurnal cycle of NOOA strongly correlated with nitrate and ammonium in NR-PM (r > 0.93) whereas OOA-1 exhibited a bimodal pattern that was similar to sulfate in $NR\text{-}PM_{rBC}$ (Figure 5g). The bimodal pattern suggests that the formation mechanisms of OOA-1 in the morning and afternoon may be slightly different but they cannot be separated by PMF due to their chemical similarity. Assuming a certain fraction of OOA-1 was produced through photochemistry by following the diurnal pattern of OOA-2, mass loadings of OOA-1 in the morning and afternoon peaks can be roughly estimated as illustrated by the red dashed lines in Figure 5g. The estimated OOA-1 peak in the morning matches reasonably well with the NH_4NO_3 and NOOA peaks, suggesting OOA-1 observed in the morning may be related to nitrate formation chemistry. Furthermore, the estimation yields that the production rate of OOA-1 in the afternoon was comparable to that of OOA-2 and the peak mass loadings of VOOA were about 5 times higher than the total of OOA-1 and OOA-2 (Figure 5g and 5h). Overall, approximately 20 wt% of OOA components were estimated to be internally mixed with rBC on average (Figure 6).

A key question remaining is whether the OOA materials identified by the SP-AMS and HR-ToF-AMS are the same in terms of AMS mass spectral characteristics. Figures 3 and S6 show that the mass spectra of OOA factors measured by the two instruments were clearly distinct from each other. Specifically, VOOA and NOOA were dominated by an organic fragment of CO_2^+ (i.e. a tracer of organic acids) and $C_2H_3O^+$ followed by CHO^+, respectively whereas $C_2H_3O^+$ was the major fragment of OOA-1 and OOA-2. However, it is particularly important to point out that different aerosol vaporization schemes utilized in SP-AMS and HR-ToF-AMS makes the direct comparison of organic mass spectra not straightforward. It has been demonstrated that thermal vaporization (operated at 600°C) used in the HR-ToF-AMS produces significant decomposition and dehydration of oxidized organic compounds (Canagaratna et al., 2015a) but the laser vaporization used in SP-AMS can provide soft vaporization of organic coatings on rBC particles at lower temperature, resulting in less molecular fragmentation (Canagaratna et al., 2015b). The OOA-1 and OOA-2 spectra notably have more peaks and with higher intensities at larger m/z (> 60 amu) compared to the NOOA and VOOA spectra. Also, the relative intensity of the peaks at m/z 28 and 29 (CO^+ and CHO^+ respectively) are substantially reduced in the OOA-1 and OOA-2 spectra compared to NOOA and VOOA. Both of these observations are consistent with reduced fragmentation from vaporization in the SP-AMS being a major reason for the differences.

Deleted: CH_2O^+

Deleted: m/z 28, 29 and 30 (CO^+, CHO^+ and CH_2O^+, respectively)

The elemental ratios (O/C and H/C) extracted from the SP-AMS and HR-ToF-AMS mass spectra of oxidized organic species have been shown to be different. Canagaratna et al. (2015b) reported that the SP-AMS O/C and H/C values differ from their corresponding HR-ToF-AMS values by factors of 0.83 and 1.16, respectively, based on the laboratory analysis of chemical standards, including dicarboxylic acids, multifunctional acids and alcohols. These conversion factors are applied to the O/C and H/C ratios of NOOA, VOOA and $SOA_{NR\text{-}PM}$ (i.e., mass-weighted values of NOOA and VOOA) (Chen et al., 2017) in order to perform a more meaningful comparison to our SP-AMS measurements in the Van Krevelen diagram (Figure 7). The elemental ratios of SOA_{rBC} and $SOA_{NR\text{-}PM}$ are comparable to each other, well within the measurement uncertainties. Similar observations are obtained between OOA-2 and VOOA. In contrast, the O/C and H/C ratios of OOA-1 are rather different to the adjusted values of NOOA, VOOA and $SOA_{NR\text{-}PM}$, suggesting some chemical difference between OOA-1 and those SOA materials. This is also consistent with the fact that OOA-1 mass concentrations increased faster than other OOA materials in the morning. More field and laboratory data are required to validate and improve the empirical relationships proposed by Canagaratna et al., (2015b) and to understand the extent to which the observed differences are a result of true chemical differences versus explainable by differences in molecular fragmentation due to the different vaporization schemes used in the instruments.

Deleted: These conversion factors are applied to the O/C and H/C ratios of NOOA and VOOA (Chen et al., 2017) in order to perform a more meaningful comparison to our SP-AMS measurements in the Van Krevelen diagram (Figure 7). The O/C and H/C ratios of OOA-2 are similar to those of VOOA (0.62 vs. 0.66 and 1.63 vs. 1.67, respectively), well within the measurement uncertainties. The O/C of OOA-1 is lower than the adjusted O/C of either NOOA or VOOA, suggesting some chemical difference between OOA-1 and the externally mixed SOA. However, the non-weighted average of the adjusted H/C for NOOA and VOOA (H/C_{avg} = 1.97) is very similar to that of OOA-1 (H/C = 1.93).

4. Conclusions and Atmospheric Implications

The repeated diurnal patterns of inorganic species, POA and SOA reported here provide a unique opportunity to investigate the chemical characteristics and formation of OA coating on rBC particles near traffic emissions. There is no doubt that HOA was internally mixed with rBC significantly as they were largely co-emitted by vehicles. The results of PMF illustrate that rBC- and HOA-rich factors accounted for about 60 and 20 wt% of rBC with thin coating, respectively, and the rBC-rich factor contributed about 82 wt% of the freshly emitted rBC from traffic, similar to previous observation in the roadside environment

(Willis et al., 2016). The COA factor is commonly observed in urban areas (Allan et al., 2010;Mohr et al., 2012) but its mixing with ambient rBC is seldom reported. The absence of a COA factor in rBC-containing particles highlights the fact that emissions of rBC from modern kitchens and the mixing of rBC and COA through particle coalescence were negligible in this study. Previous measurements conducted in an urban area also pointed to the same conclusion (Lee et al., 2015;Willis et al., 2016).

Increases in coating thickness were primarily due to substantial formation of fresh SOA through local photochemical processing on the timescale of a few hours. On average, about 7-20 wt% of secondary aerosol species, including both inorganic and OOA species, were condensed on rBC particles, suggesting that rBC was unlikely the major sink for condensation of fresh SOA in this study. During the peak of SOA production, the average mass loadings of rBC and VOOA were about 0.2 and 4 μg/m^3, respectively, which were a few factors to orders of magnitude lower than those generated in some recent aging experiments of soot particles (Metcalf et al., 2013;Li et al., 2017). Peng et al. (2016) recently showed that the timescale for producing sufficient fresh SOA to completely modify rBC properties strongly depends on pollution levels. Our observations may provide insight into the design of soot aging experiments for investigating the formation rate of fresh SOA coatings (e.g., growth rate of coating thickness) as well as their environmental impacts under a more atmospherically relevant condition.

Deleted: 0.2 and 6.8

Our measurement approach leads to a conclusion that at least a fraction of OOA condensed on rBC was chemically distinct from that externally mixed with rBC, although uncertainties of organic fragmentation due to the application of the laser vaporizer still need to be fully established to quantify this difference. The reason for this unique observation remains unclear. One of the possibilities is that SOA$_{rBC}$ formed more locally on shorter timescales (e.g., photo-oxidation of anthropogenic volatile organic compounds (VOCs) near traffic emissions) could preferentially condense onto rBC particles in Aiken mode that can provide a larger overall surface area to the condensing gases compared to other existing background particles. The more oxidized OOA materials formed regionally on longer timescales (e.g., a fraction of VOOA that were largely externally mixed with rBC) under conditions with relatively low concentrations of (or without) rBC particle could be advected to the sampling region during the day. Furthermore, atmospheric dilution of traffic emissions can modify the chemical compositions and concentrations of SOA precursors and seed particles so that the formation of secondary coatings on rBC might be less efficient and chemically different under diluted conditions (e.g., after boundary layer break up and mixing with air masses from residual layer). This may partially explain the formation of VOOA in SOA$_{NR-PM}$ through local photochemistry. There may also be a mechanistic preference for material to condense onto certain surfaces because of their chemical nature (e.g., hydrophobic coating (e.g. HOA and soot surface functionality) but future research efforts are required to explore this possibility further.

Deleted: One possibility is that SOA production via photooxidation of anthropogenic volatile organic compounds (VOCs) started occurring near traffic emission sources in which relatively high concentrations of rBC particles played a more critical role for SOA condensation compared to other existing background particles.

Deleted: In particular, certain classes of SOA precursors may oxidize more rapidly or require less oxidation steps (e.g., Intermediate VOCs vs. VOCs) to low-volatility organics than the others, forming a different type of SOA near emissions and further downfield. Atmospheric dilution modified the chemical compositions and concentrations of SOA precursors and seed particles so that the formation of coatings on rBC might be less efficient and chemically different under the diluted conditions. For example, VOOA formation in the late afternoon linked to the transport and formation chemistry of inorganic sulfate, which was probably less relevant to the formation of OOA coating on rBC. Research efforts are required to examine whether certain SOA materials are more favorable to condense on rBC-containing particles compared to other types of seed particles. The roles of hydrophobic coating (e.g. HOA) and soot surface functionality on SOA condensation need to be further explored.

Acknowledgements

Lee A. K. Y. would like to acknowledge the support from the NUS Start-up Grant (R-302-000-173-133). Cappa D. C. and Russell L. M. were supported by the California Air Resources Board (Agreement number: 13-330)The authors would also like to thank the Fontana Fire Department and the South Coast Air Quality Management District (SCAQMD) for Fontana site logistics.

References

Allan, J. D., Delia, A. E., Coe, H., Bower, K. N., Alfarra, M. R., Jimenez, J. L., Middlebrook, A. M., Drewnick, F., Onasch, T. B., Canagaratna, M. R., Jayne, J. T., and Worsnop, D. R.: A generalised method for the extraction of chemically resolved mass spectra from aerodyne aerosol mass spectrometer data, J.Aerosol Sci., 35, 909, 10.1016/j.jaerosci.2004.02.007, 2004.

Allan, J. D., Williams, P. I., Morgan, W. T., Martin, C. L., Flynn, M. J., Lee, J., Nemitz, E., Phillips, G. J., Gallagher, M. W., and Coe, H.: Contributions from transport, solid fuel burning and cooking to primary organic aerosols in two UK cities, Atmospheric Chemistry and Physics, 10, 647-668, 10.5194/acp-10-647-2010, 2010.

Betha, R., Russell, L. M., Chen, C.-L., Liu, J., Price, D. J., Sanchez, K. J., Chen, S., Lee A. K. Y., Collier, S. C., Zhang, Q., Zhang, X., and Cappa, C. D.: Larger submicron particles for emissions with residential burning in wintertime San Joaquin Valley (Fresno) than for vehicle combustion in summertime South Coast Air Basin (Fontana), under review.

Bond, T. C., Doherty, S. J., Fahey, D. W., Forster, P. M., Berntsen, T., DeAngelo, B. J., Flanner, M. G., Ghan, S., Karcher, B., Koch, D., Kinne, S., Kondo, Y., Quinn, P. K., Sarofim, M. C., Schultz, M. G., Schulz, M., Venkataraman, C., Zhang, H., Zhang, S., Bellouin, N., Guttikunda, S. K., Hopke, P. K., Jacobson, M. Z., Kaiser, J. W., Klimont, Z., Lohmann, U., Schwarz, J. P., Shindell, D., Storelvmo, T., Warren, S. G., and Zender, C. S.: Bounding the role of black carbon in the climate system: A scientific assessment, Journal of Geophysical Research-Atmospheres, 118, 5380-5552, 10.1002/jgrd.50171, 2013.

Brown, S. S., Talukdar, R. K., and Ravishankara, A. R.: Rate constants for the reaction OH+NO2+M -> HNO3+M under atmospheric conditions, Chemical Physics Letters, 299, 277-284, 10.1016/s0009-2614(98)01283-4, 1999.

Canagaratna, M. R., Jayne, J. T., Jimenez, J. L., Allan, J. D., Alfarra, M. R., Zhang, Q., Onasch, T. B., Drewnick, F., Coe, H., Middlebrook, A., Delia, A., Williams, L. R., Trimborn, A. M., Northway, M. J., DeCarlo, P. F., Kolb, C. E., Davidovits, P., and Worsnop, D. R.: Chemical and microphysical characterization of ambient aerosols with the aerodyne aerosol mass spectrometer, Mass Spectrometry Reviews, 26, 185-222, 10.1002/mas.20115, 2007.

Canagaratna, M. R., Jimenez, J. L., Kroll, J. H., Chen, Q., Kessler, S. H., Massoli, P., Ruiz, L. H., Fortner, E., Williams, L. R., Wilson, K. R., Surratt, J. D., Donahue, N. M., Jayne, J. T., and Worsnop, D. R.: Elemental ratio measurements of organic compounds using aerosol mass spectrometry: characterization, improved calibration, and implications, Atmospheric Chemistry and Physics, 15, 253, 10.5194/acp-15-253-2015, 2015a.

Canagaratna, M. R., Massoli, P., Browne, E. C., Franklin, J. P., Wilson, K. R., Onasch, T. B., Kirchstetter, T. W., Fortner, E. C., Kolb, C. E., Jayne, J. T., Kroll, J. H., and Worsnop, D. R.: Chemical Compositions of Black Carbon Particle Cores and Coatings via Soot Particle Aerosol Mass Spectrometry with Photoionization and Electron Ionization, Journal of Physical Chemistry A, 119, 4589-4599, 10.1021/jp510711u, 2015b.

Cappa, C. D., Onasch, T. B., Massoli, P., Worsnop, D. R., Bates, T. S., Cross, E. S., Davidovits, P., Hakala, J., Hayden, K. L., Jobson, B. T., Kolesar, K. R., Lack, D. A., Lerner, B. M., Li, S. M., Mellon, D., Nuaaman, I., Olfert, J. S., Petaja, T., Quinn, P. K., Song, C., Subramanian, R., Williams, E. J., and Zaveri, R. A.: Radiative Absorption Enhancements Due to the Mixing State of Atmospheric Black Carbon, Science, 337, 1078-1081, 10.1126/science.1223447, 2012.

Corbin, J. C., Sierau, B., Gysel, M., Laborde, M., Keller, A., Kim, J., Petzold, A., Onasch, T. B., Lohmann, U., and Mensah, A. A.: Mass spectrometry of refractory black carbon particles from six sources: carbon-cluster and oxygenated ions, Atmospheric Chemistry and Physics, 14, 2591-2603, 10.5194/acp-14-2591-2014, 2014.

Chen, C.-L., Chen, S., Russell, L. M., Liu, J., Price, D. J., Betha, R., Sanchez, K. J., Lee A. K. Y., Collier, S. C., Zhang, Q., Kumar, A., Kleeman, M., Zhang, X., and Cappa, C. D.: Organic aerosol particle chemical properties associated with residential burning and fog in wintertime San Joaquin Valley (Fresno) and with vehicle and firework emissions in summertime South Coast Air Basin (Fontana), Under review.

DeCarlo, P. F., Slowik, J. G., Worsnop, D. R., Davidovits, P., and Jimenez, J. L.: Particle morphology and density characterization by combined mobility and aerodynamic diameter measurements. Part 1: Theory, Aerosol Science and Technology, 38, 1185-1205, 10.1080/027868290903907, 2004.

DeCarlo, P. F., Kimmel, J. R., Trimborn, A., Northway, M. J., Jayne, J. T., Aiken, A. C., Gonin, M., Fuhrer, K., Horvath, T., Docherty, K. S., Worsnop, D. R., and Jimenez, J. L.: Field-deployable, high-resolution, time-of-flight aerosol mass spectrometer, Anal.Chem., 78, 8281, 10.1021/ac061249n, 2006.

Enroth, J., Saarikoski, S., Niemi, J., Kousa, A., Jezek, I., Mocnik, G., Carbone, S., Kuuluvainen, H., Ronkko, T., Hillamo, R., and Pirjola, L.: Chemical and physical characterization of traffic particles in four different highway environments in the Helsinki metropolitan area, Atmospheric Chemistry and Physics, 16, 5497-5512, 10.5194/acp-16-5497-2016, 2016.

Gentner, D. R., Jathar, S. H., Gordon, T. D., Bahreini, R., Day, D. A., El Haddad, I., Hayes, P. L., Pieber, S. M., Platt, S. M., de Gouw, J., Goldstein, A. H., Harley, R. A., Jimenez, J. L., Prevot, A. S. H., and Robinson, A. L.: Review of Urban Secondary Organic Aerosol Formation from Gasoline and Diesel Motor Vehicle Emissions, Environmental Science & Technology, 51, 1074-1093, 10.1021/acs.est.6b04509, 2017.

Guo, S., Hu, M., Lin, Y., Gomez-Hernandez, M., Zamora, M. L., Peng, J. F., Collins, D. R., and Zhang, R. Y.: OH-Initiated Oxidation of m-Xylene on Black Carbon Aging, Environmental Science & Technology, 50, 8605-8612, 10.1021/acs.est.6b01272, 2016.

Jacobson, M. Z.: Strong radiative heating due to the mixing state of black carbon in atmospheric aerosols, Nature, 409, 695-697, 10.1038/35055518, 2001.

Jimenez, J. L., Jayne, J. T., Shi, Q., Kolb, C. E., Worsnop, D. R., Yourshaw, I., Seinfeld, J. H., Flagan, R. C., Zhang, X. F., Smith, K. A., Morris, J. W., and Davidovits, P.: Ambient aerosol sampling using the Aerodyne Aerosol Mass Spectrometer, Journal of Geophysical Research-Atmospheres, 108, 10.1029/2001jd001213, 2003.

Kroll, J. H., Donahue, N. M., Jimenez, J. L., Kessler, S. H., Canagaratna, M. R., Wilson, K. R., Altieri, K. E., Mazzoleni, L. R., Wozniak, A. S., Bluhm, H., Mysak, E. R., Smith, J. D., Kolb, C. E., and Worsnop, D. R.: Carbon oxidation state as a metric for describing the chemistry of atmospheric organic aerosol, Nature Chemistry, 3, 133-139, 10.1038/nchem.948, 2011.

Kuwata, M., Kondo, Y., and Takegawa, N.: Critical condensed mass for activation of black carbon as cloud condensation nuclei in Tokyo, Journal of Geophysical Research-Atmospheres, 114, 10.1029/2009jd012086, 2009.

Laborde, M., Crippa, M., Tritscher, T., Juranyi, Z., Decarlo, P. F., Temime-Roussel, B., Marchand, N., Eckhardt, S., Stohl, A., Baltensperger, U., Prevot, A. S. H., Weingartner, E., and Gysel, M.: Black carbon physical properties and mixing state in the European megacity Paris, Atmospheric Chemistry and Physics, 13, 5831-5856, 10.5194/acp-13-5831-2013, 2013.

Lee, A. K. Y., Willis, M. D., Healy, R. M., Onasch, T. B., and Abbatt, J. P. D.: Mixing state of carbonaceous aerosol in an urban environment: single particle characterization using the soot particle aerosol mass spectrometer (SP-AMS), Atmospheric Chemistry and Physics, 15, 1823-1841, 10.5194/acp-15-1823-2015, 2015.

Lee, A. K. Y., Willis, M. D., Healy, R. M., Wang, J. M., Jeong, C. H., Wenger, J. C., Evans, G. J., and Abbatt, J. P. D.: Single-particle characterization of biomass burning organic aerosol (BBOA): evidence for non-uniform mixing of high molecular weight organics and potassium, Atmospheric Chemistry and Physics, 16, 5561-5572, 10.5194/acp-16-5561-2016, 2016.

Li, K. W., Chen, L. H., Han, K., Lv, B. A., Bao, K. J., Wu, X. C., Gao, X., and Cen, K. F.: Smog chamber study on aging of combustion soot in isoprene/SO2/NOx system: Changes of mass, size, effective density, morphology and mixing state, Atmospheric Research, 184, 139-148, 10.1016/j.atmosres.2016.10.011, 2017.

Liu, D., Allan, J., Whitehead, J., Young, D., Flynn, M., Coe, H., McFiggans, G., Fleming, Z. L., and Bandy, B.: Ambient black carbon particle hygroscopic properties controlled by mixing state and composition, Atmospheric Chemistry and Physics, 13, 2015-2029, 10.5194/acp-13-2015-2013, 2013.

Liu, D. T., Whitehead, J., Alfarra, M. R., Reyes-Villegas, E., Spracklen, D. V., Reddington, C. L., Kong, S. F., Williams, P. I., Ting, Y. C., Haslett, S., Taylor, J. W., Flynn, M. J., Morgan, W. T., McFiggans, G., Coe, H., and Allan, J. D.: Black-carbon absorption enhancement in the atmosphere determined by particle mixing state, Nature Geoscience, 10, 184-U132, 10.1038/ngeo2901, 2017.

Liu, S., Aiken, A. C., Gorkowski, K., Dubey, M. K., Cappa, C. D., Williams, L. R., Herndon, S. C., Massoli, P., Fortner, E. C., Chhabra, P. S., Brooks, W. A., Onasch, T. B., Jayne, J. T., Worsnop, D. R., China, S., Sharma, N., Mazzoleni, C., Xu, L., Ng, N. L., Liu, D., Allan, J. D., Lee, J. D., Fleming, Z. L., Mohr, C., Zotter, P., Szidat, S., and Prevot, A. S. H.: Enhanced light absorption by mixed source black and brown carbon particles in UK winter, Nature Communications, 6, 10.1038/ncomms9435, 2015.

Malmborg, V. B., Eriksson, A. C., Shen, M., Nilsson, P., Gallo, Y., Waldheim, B., Martinsson, J., Andersson, O., and Pagels, J.: Evolution of In-Cylinder Diesel Engine Soot and Emission Characteristics Investigated with Online Aerosol Mass Spectrometry, Environmental Science & Technology, 51, 1876-1885, 10.1021/acs.est.6b03391, 2017.

Massoli, P., Fortner, E. C., Canagaratna, M. R., Williams, L. R., Zhang, Q., Sun, Y., Schwab, J. J., Trimborn, A., Onasch, T. B., Demerjian, K. L., Kolb, C. E., Worsnop, D. R., and Jayne, J. T.: Pollution Gradients and Chemical Characterization of Particulate Matter from Vehicular Traffic near Major Roadways: Results from the 2009 Queens College Air Quality Study in NYC, Aerosol Science and Technology, 46, 1201-1218, 10.1080/02786826.2012.701784, 2012.

Massoli, P., Onasch, T. B., Cappa, C. D., Nuamaan, I., Hakala, J., Hayden, K., Li, S. M., Sueper, D. T., Bates, T. S., Quinn, P. K., Jayne, J. T., and Worsnop, D. R.: Characterization of black carbon-containing particles from soot particle aerosol mass spectrometer measurements on the R/V Atlantis during CalNex 2010, Journal of Geophysical Research-Atmospheres, 120, 2575-2593, 10.1002/2014jd022834, 2015.

McMeeking, G. R., Good, N., Petters, M. D., McFiggans, G., and Coe, H.: Influences on the fraction of hydrophobic and hydrophilic black carbon in the atmosphere, Atmospheric Chemistry and Physics, 11, 5099-5112, 10.5194/acp-11-5099-2011, 2011.

Metcalf, A. R., Loza, C. L., Coggon, M. M., Craven, J. S., Jonsson, H. H., Flagan, R. C., and Seinfeld, J. H.: Secondary Organic Aerosol Coating Formation and Evaporation: Chamber Studies Using Black Carbon Seed Aerosol and the Single-Particle Soot Photometer, Aerosol Science and Technology, 47, 326-347, 10.1080/02786826.2012.750712, 2013.

Moffet, R. C., and Prather, K. A.: In-situ measurements of the mixing state and optical properties of soot with implications for radiative forcing estimates, Proceedings of the National Academy of Sciences of the United States of America, 106, 11872-11877, 10.1073/pnas.0900040106, 2009.

Mohr, C., DeCarlo, P. F., Heringa, M. F., Chirico, R., Slowik, J. G., Richter, R., Reche, C., Alastuey, A., Querol, X., Seco, R., Penuelas, J., Jimenez, J. L., Crippa, M., Zimmermann, R., Baltensperger, U., and Prevot, A. S. H.: Identification and quantification of organic aerosol from cooking and other sources in Barcelona using aerosol mass spectrometer data, Atmospheric Chemistry and Physics, 12, 1649-1665, 10.5194/acp-12-1649-2012, 2012.

Onasch, T. B., Trimborn, A., Fortner, E. C., Jayne, J. T., Kok, G. L., Williams, L. R., Davidovits, P., and Worsnop, D. R.: Soot Particle Aerosol Mass Spectrometer: Development, Validation, and Initial Application, Aerosol Science and Technology, 46, 804-817, 10.1080/02786826.2012.663948, 2012.

Paatero, P., and Tapper, U.: POSITIVE MATRIX FACTORIZATION - A NONNEGATIVE FACTOR MODEL WITH OPTIMAL UTILIZATION OF ERROR-ESTIMATES OF DATA VALUES, Environmetrics, 5, 111-126, 10.1002/env.3170050203, 1994.

Peng, J. F., Hu, M., Guo, S., Du, Z. F., Zheng, J., Shang, D. J., Zamora, M. L., Zeng, L. M., Shao, M., Wu, Y. S., Wang, Y., Glen, C. R., Collins, D. R., Molina, M. J., and Zhang, R. Y.: Markedly enhanced absorption and direct radiative forcing of black carbon under polluted urban environments, Proceedings of the National Academy of Sciences of the United States of America, 113, 4266-4271, 10.1073/pnas.1602310113, 2016.

Ramanathan, V., and Carmichael, G.: Global and regional climate changes due to black carbon, Nature Geoscience, 1, 221-227, 10.1038/ngeo156, 2008.

Saarikoski, S., Timonen, H., Carbone, S., Kuuluvainen, H., Niemi, J. V., Kousa, A., Ronkko, T., Worsnop, D., Hillamo, R., and Pirjola, L.: Investigating the chemical species in submicron particles emitted by city buses, Aerosol Science and Technology, 51, 317-329, 10.1080/02786826.2016.1261992, 2017.

Schnitzler, E. G., Dutt, A., Charbonneau, A. M., Olfert, J. S., and Jager, W.: Soot Aggregate Restructuring Due to Coatings of Secondary Organic Aerosol Derived from Aromatic Precursors, Environmental Science & Technology, 48, 14309-14316, 10.1021/es503699b, 2014.

Slowik, J. G., Brook, J., Chang, R. Y.-W., Evans, G. J., Hayden, K., Jeong, C.-H., Li, S.-M., Liggio, J., Liu, P. S. K., McGuire, M., Mihele, C., Sjostedt, S., Vlasenko, A., and Abbatt, J. P. D.: Photochemical processing of organic aerosol at nearby continental sites: contrast between urban plumes and regional aerosol, Atmos. Chem. Phys., 11, 2991-3006, doi:10.5194/acp-11-2991-2011, 2011.

Takegawa, N., Miyakawa, T., Kondo, Y., Blake, D. R., Kanaya, Y., Koike, M., Fukuda, M., Komazaki, Y., Miyazaki, Y., Shimono, A., and Takeuchi, T.: Evolution of submicron organic aerosol in polluted air exported from Tokyo, Geophysical Research Letters, 33, 10.1029/2006gl025815, 2006.

Tkacik, D. S., Lambe, A. T., Jathar, S., Li, X., Presto, A. A., Zhao, Y. L., Blake, D., Meinardi, S., Jayne, J. T., Croteau, P. L., and Robinson, A. L.: Secondary Organic Aerosol Formation from in-Use Motor Vehicle Emissions Using a Potential Aerosol Mass Reactor, Environmental Science & Technology, 48, 11235-11242, 10.1021/es502239v, 2014.

Ulbrich, I. M., Canagaratna, M. R., Zhang, Q., Worsnop, D. R., and Jimenez, J. L.: Interpretation of organic components from Positive Matrix Factorization of aerosol mass spectrometric data, Atmospheric Chemistry and Physics, 9, 2891-2918, 10.5194/acp-9-2891-2009, 2009.

Wang, Q. Y., Huang, R. J., Zhao, Z. Z., Cao, J. J., Ni, H. Y., Tie, X. X., Zhu, C. S., Shen, Z. X., Wang, M., Dai, W. T., Han, Y. M., Zhang, N. N., and Prevot, A. S. H.: Effects of photochemical oxidation on the mixing state and light absorption of black carbon in the urban atmosphere of China, Environmental Research Letters, 12, 10.1088/1748-9326/aa64ea, 2017.

Willis, M. D., Lee, A. K. Y., Onasch, T. B., Fortner, E. C., Williams, L. R., Lambe, A. T., Worsnop, D. R., and Abbatt, J. P. D.: Collection efficiency of the soot-particle aerosol mass spectrometer (SP-AMS) for internally mixed particulate black carbon, Atmospheric Measurement Techniques, 7, 4507-4516, 10.5194/amt-7-4507-2014, 2014.

Willis, M. D., Healy, R. M., Riemer, N., West, M., Wang, J. M., Jeong, C. H., Wenger, J. C., Evans, G. J., Abbatt, J. P. D., and Lee, A. K. Y.: Quantification of black carbon mixing state from traffic: implications for aerosol optical properties, Atmospheric Chemistry and Physics, 16, 4693-4706, 10.5194/acp-16-4693-2016, 2016.

Zhang, Q., Jimenez, J. L., Canagaratna, M. R., Ulbrich, I. M., Ng, N. L., Worsnop, D. R., and Sun, Y. L.: Understanding atmospheric organic aerosols via factor analysis of aerosol mass spectrometry: a review, Analytical and Bioanalytical Chemistry, 401, 3045-3067, 10.1007/s00216-011-5355-y, 2011.

Figures

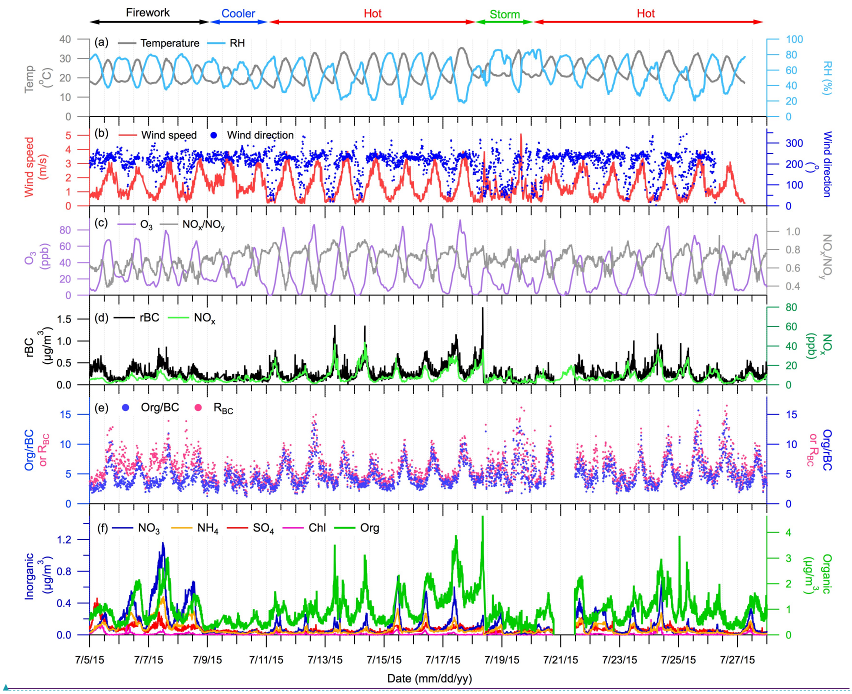

Figure 1: Time series of (a) temperature and RH, (b) wind speed and direction, (c) ozone and NO_x/NO_y ratio, (d) rBC and NO_x, (e) Org/rBC ratio and R_{BC}, and (f) $NR\text{-}PM_{rBC}$ (NO3 = nitrate, NH4 = ammonium, SO4 = sulfate, Chl = chloride and Org = organic)

Formatted: Font:10 pt

Formatted: Font:10 pt

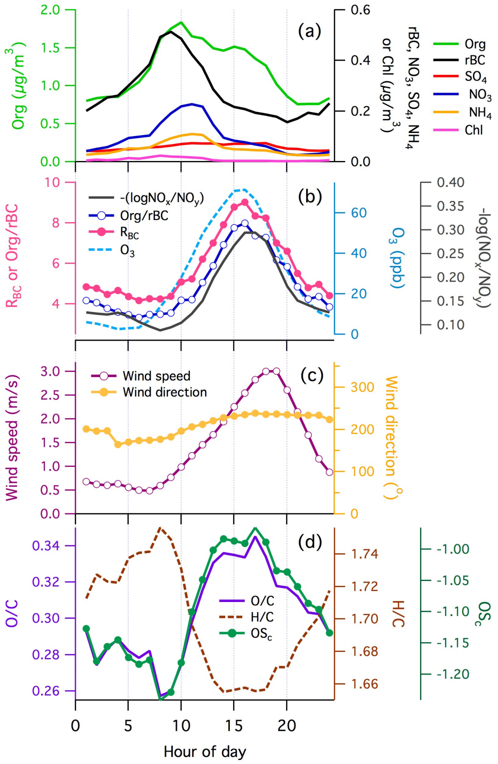

Figure 2: Diurnal cycles of (a) rBC and NR-PM$_{rBC}$, (b) Org/rBC ratio, R_{BC}, ozone and –log (NO_x/NO_y), (c) wind speed and direction, and (d) O/C, H/C and OS within the hot period (See Figure S7 for the uncertainties of data)

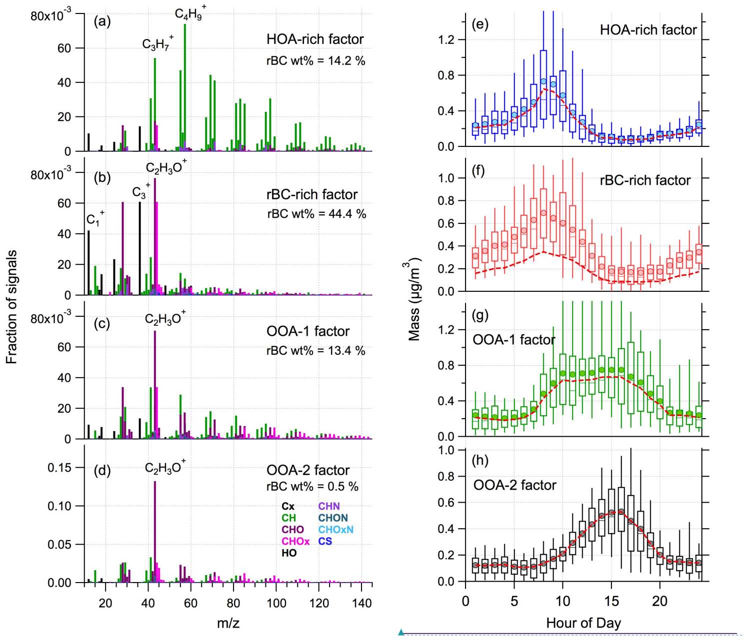

Formatted: Font:10 pt

Figure 3: Mass spectra (a-d) and diurnal cycles (e-h) of PMF factors from SP-AMS data within the hot period. (Box plots: 5th, 25th, 50th, 75th and 95th percentile, Filled circles: mean values for organic + C_x^+ fragments, Red dashed lines: mean values for organic alone. RIE of 0.26 and 1.4 were applied for rBC and organic fragments, respectively, for the diurnal patterns.)

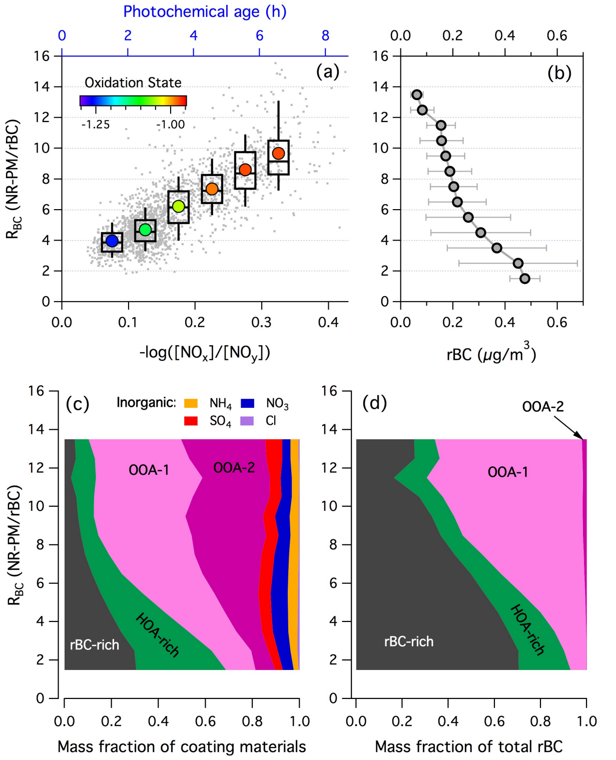

Formatted: Font:10 pt

Figure 4: Coating thickness (R_{BC}) as a function of (a) photochemical age, (b) rBC mass loadings, (c) chemical compositions of coating, and (d) rBC mass fractions contributed by individual PMF factors within the hot period

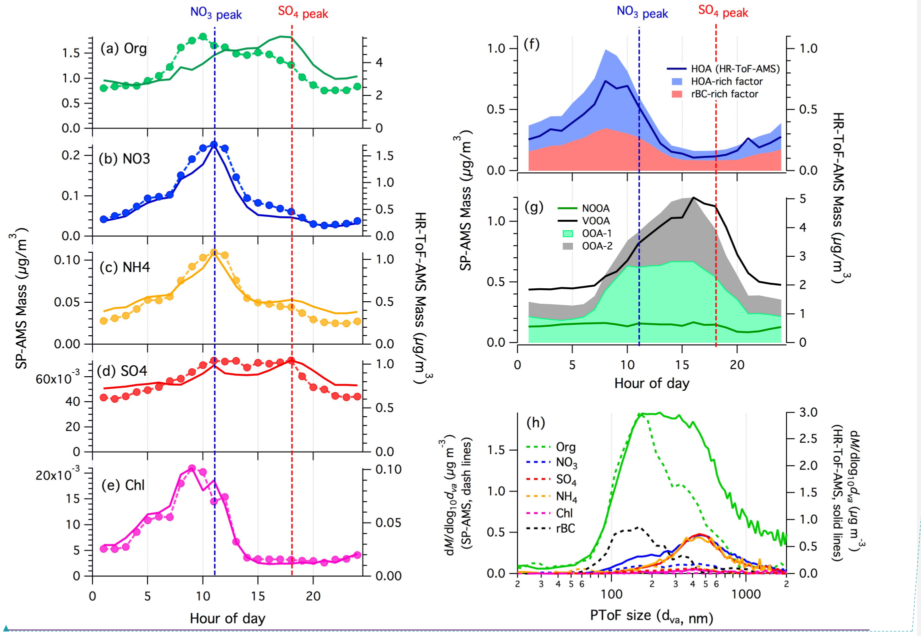

Formatted: Font:10 pt

Figure 5: (a-e) Diurnal cycles of NR-PM and NR-PM$_{rBC}$ measured by HR-ToF-AMS (solid lines) and SP-AMS (dashed lines with circles), respectively. (f-g) Diurnal cycles of PMF factors from HR-ToF-AMS (solid lines) and SP-AMS (filled areas, organics components only for PMF factors) data. (h) PToF size distribution of rBC, NR-PM (dashed lines) and NR-PM$_{rBC}$ (solid lines).

Deleted: h

Deleted: i

Deleted: Mass loadings of OOA-1 in the morning and afternoon peaks can be roughly estimated as illustrated by the red dashed lines in panel g assuming OOA-1 was produced through photochemistry by following the diurnal pattern of OOA-2 in the afternoon.

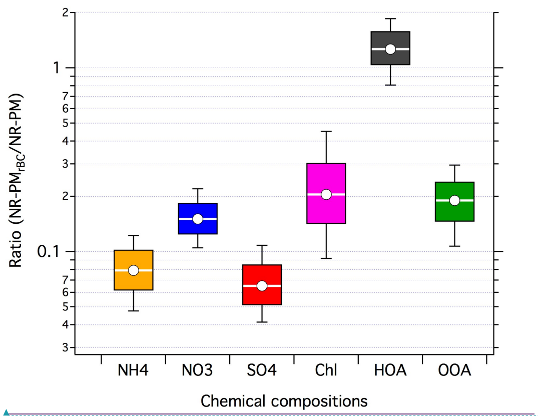

Formatted: Font:10 pt

Figure 6: NR-PM$_{rBC}$-to-NR-PM ratios for individual aerosol components and PMF factors (Box plots: 10th, 25th, 50th, 75th and 90th percentile, White circles: mean values, OOA = ([OOA-1] + [OOA-2]) / ([NOOA] + [VOOA]) = SOA$_{rBC}$ / SOA$_{NR-PM}$ and HOA = ([HOA-rich] + [rBC-rich]) / [HOA]). Only organics components for PMF factors measured by SP-AMS were used in this calculation. HOA loadings less than 0.15 µg/m^3 from HR-ToF-AMS were removed for the calculation.

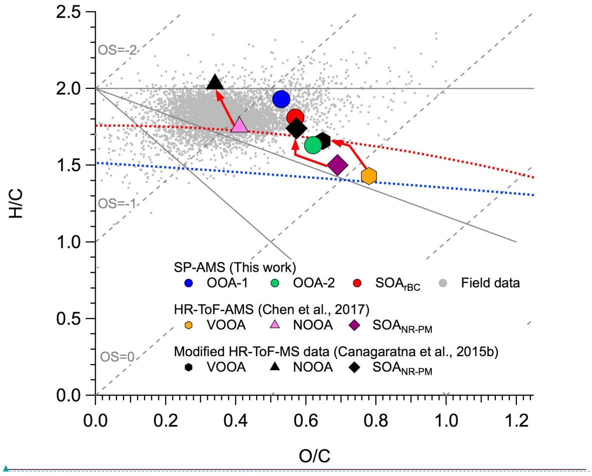

Formatted: Font:10 pt

Figure 7: Van Krevelen diagram: Red arrows indicate the changes in the elemental ratios of VOOA, NOOA factors and SOA$_{NR-PM}$ measured by the HR-ToF-AMS after applying the correction factors for more oxygenated organic species proposed by Canagaratna et al. (2015b).